LU TP 15-11
July 2015

Diffractive bremsstrahlung in hadronic collisions

Roman Pasechnik*

Department of Astronomy and Theoretical Physics,
Lund University, SE 223-62 Lund, Sweden

Boris Kopeliovich† and Irina Potashnikova‡

Departamento de Física, Universidad Técnica Federico Santa María; and
Centro Científico-Tecnológico de Valparaíso,
Avda. España 1680, Valparaíso, Chile

Abstract

Production of heavy photons (Drell-Yan), gauge bosons, Higgs bosons, heavy flavors, which is treated within the QCD parton model as a result of hard parton-parton collision, can be considered as a bremsstrahlung process in the target rest frame. In this review, we discuss the basic features of the diffractive channels of these processes in the framework of color dipole approach. The main observation is a dramatic breakdown of diffractive QCD factorisation due to the interplay between soft and hard interactions, which dominates these processes. This observation is crucial for phenomenological studies of diffractive reactions in high-energy hadronic collisions.

PACS numbers: 13.87.Ce, 14.65.Dw, 14.80.Bn

*Electronic address: Roman.Pasechnik@thep.lu.se
†Electronic address: boris.kopeliovich@usm.cl
‡Electronic address: irina.potashnikova@usm.cl

I. INTRODUCTION

Diffractive production of particles in hadron-hadron scattering at high energies is one of the basic tools, experimental and theoretical, giving access to small-x and nonperturbative QCD physics. The characteristic feature of diffractive processes at high energies is the presence of a large rapidity gap between the remnants of the beam and target.

The understanding of the mechanisms of inelastic diffraction came with the pioneering works of Glauber [1], Feinberg and Pomeranchuk [2], Good and Walker [3]. Here diffraction is conventionally viewed as a shadow of inelastic processes. If the incoming plane wave contains components interacting differently with the target, the outgoing wave will have a different composition, i.e. besides elastic scattering a new *diffractive* state will be created resulting in a new combination of the Fock components (for a detailed review on QCD diffraction, see Ref. [4, 5]). Diffraction, which is usually a soft process, is difficult to predict from the first principles, because it involves poorly known nonperturbative effects. Therefore, diffractive reactions characterised by a hard scale deserve a special attention. It is tempting, on analogy to inclusive reactions, to expect that QCD factorization holds for such diffractive processes. Although factorization of short and long distances still holds in diffractive DIS, the fracture functions are not universal and cannot be used for other diffractive processes.

Examples of breakdown of diffractive factorization are the processes of production of Drell-Yan dileptons [6, 7], gauge bosons [8] and heavy flavors [9]. Factorization turns out to be broken in all these channels in spite of presence of a hard scale given by the large masses of produced particles, it occurs due to the interplay of short- and long-range interactions.

The main difficulty in formulation of a theoretical QCD-based framework for diffractive scattering is caused by the essential contamination of soft, non-perturbative interactions. For example, diffractive deep-inelastic scattering (DIS), $\gamma^* p \to \bar{q}qp$, although it is a higher twist process, is dominated by soft interactions [10]. Within the dipole approach [11] such a process looks like a linear combination of elastic scattering amplitudes for $\bar{q}q$ dipoles of different sizes. Although formally the process $\gamma^* \to \bar{q}q$ is an off-diagonal diffraction, it does not vanish in the limit of unitarity saturation, the so called black-disc limit. This happens because the initial and final $\bar{q}q$ distribution functions are not orthogonal. Similar features exhibit the contribution of higher Fock components of the photon, e.g. the leading twist diffraction $\gamma^* \to \bar{q}qg$.

Diffractive excitation of the beam hadron has been traditionally used as a way to measure the Pomeron-hadron total cross section [4]. This idea extended to DIS, allows to measure the structure function of the Pomeron [12]. The next step, which might look natural, is to assume that QCD factorization holds for diffraction, and to employ the extracted parton distributions in the Pomeron in order to predict the hard diffraction cross sections in hadronic collisions. However, such predictions for hard hadronic diffraction, e.g. high-p_T dijet production, failed by an order of magnitude [14, 15]. In this case the situation is different and more complicated, namely, factorization of small and large distances in hadronic diffraction is broken because of presence of spectator partons and due to large hadronic sizes.

The cross section of diffractive production of the W boson in $p\bar{p}$ collisions measured by the CDF experiment [16, 17], was also found to be six times smaller than what was predicted relying on factorisation and diffractive DIS data [18]. Besides, the phenomenological models based on diffractive factorisation, which are widely discussed in the literature (see e.g. Refs. [19, 20]), predict a significant increase of the ratio of the diffractive to inclusive

gauge bosons production cross sections with energy. The diffractive QCD factorisation in hadron collisions is, however, severely broken by the interplay of hard and soft dynamics, as was recently advocated in Refs. [7, 8], and this review is devoted to study of these important effects within the color dipole phenomenology.

The processes under discussion – single diffractive Drell-Yan [6, 7], diffractive radiation of vector (Z, $W^{\pm}$) bosons [8], diffractive heavy flavor production [9] and diffractive associated heavy flavor and Higgs boson production [21] – correspond to off-diagonal diffraction. While diagonal diffraction is enhanced by absorption effects (in fact it is a result of absorption), the off-diagonal diffractive processes are suppressed by absorption, and even vanish in the limit of maximal absorption, i.e. in the black-disc limit.

The absorptive corrections, also known as the survival probability of rapidity gaps [22], are related to initial- and final-state interactions. Usually the survival probability is introduced into the diffractive cross section in a probabilistic way [23] and is estimated in simplified models such as eikonal, quasi-eikonal, two-channel approximations, etc.

According to the Good-Walker basic mechanism of diffraction, the off-diagonal diffractive amplitude is a linear combination of diagonal (elastic) diffractive amplitudes of different Fock components in the projectile hadron. Thus, the absorptive corrections naturally emerge at the amplitude level as a result of mutual cancellations between different elastic amplitudes. Therefore, there is no need to introduce any additional multiplicative gap survival probability factors. Within the light-cone color dipole approach [11] a diffractive process is considered as a result of elastic scattering of $\bar{q}q$ dipoles of different sizes emerging in incident Fock states. The study of the diffractive Drell-Yan reaction performed in Ref. [6] has revealed importance of soft interactions with the partons spectators, which contributes on the same footing as hard perturbative ones, and strongly violate QCD factorization.

One of the advantages of the dipole description is the possibility to calculate directly (although in a process-dependent way) the full diffractive amplitude, which contains all the absorption corrections by employing the phenomenological universal dipole cross section (or dipole elastic amplitudes) fitted to DIS data. The gap survival amplitude can be explicitly singled out as a factor from the diffractive amplitude being a superposition of dipole scatterings at different transverse separations.

Interesting, that besides interaction with the spectator projectile partons, there is another important source for diffractive factorization breaking. Even a single quark, having no spectator co-movers, cannot radiate Abelian fields (γ, Z, $W^{\pm}, H$) interacting diffractively with the target with zero transverse momentum transfer [24], i.e. in forward direction scattering. This is certainly contradicts the expectations based of diffractive factorization. In the case of a hadron beam the forward directions for the hadron and quark do not coincide, so a forward radiation is possible, but is strongly suppressed (see below).

Interaction with the spectator partons opens new possibilities for diffractive radiation in forward direction, namely the transverse momenta transferred to different partons can compensate each other. It was found in Refs. [6–8] that this contribution dominates the forward diffractive Abelian radiation cross section. This mechanism leads to a dramatic violation of diffractive QCD factorisation, which predicts diffraction to be a higher twist effect, while it turns out to be a leading twist effect due to the interplay between the soft and hard interactions. Although diffractive gluon radiation off a forward quark does not vanish due to possibility of glue-glue interaction, the diffractive factorisation breaking in non-Abelian radiation is still important.

In this review, we briefly discuss the corresponding effects whereas more details can be

found in Refs. [6–9, 21].

II. COLOR DIPOLE PICTURE OF DIFFRACTIVE EXCITATION

Single diffractive scattering and production of a new (diffractive) state, i.e. diffractive excitation, emerges as a consequence of quantum fluctuations in projectile hadron. The orthogonal hadron state $|h\rangle$ can be excited due to interactions but can be decomposed over the orthogonal and complet set of eigenstates of interactions $|\alpha\rangle$ as [11, 25, 26]

$$|h\rangle = \sum C_\alpha^h \, |\alpha\rangle \, , \qquad \hat{f}_{el}|\alpha\rangle = f_\alpha |\alpha\rangle \, , \tag{2.1}$$

where $\hat{f}_{el}$ is the elastic amplitude operator and f_α is one of its eignestates. The eigen amplitudes f_α are the same for different types of hadrons. Hence, the elastic $h \to h$ and single diffractive $h \to h'$ amplitudes can be conveniently written in terms of the elastic eigen amplitudes f_α and coefficients C_α^h, i.e.

$$f_{el}^{hh} = \sum |C_\alpha^h|^2 \, f_\alpha \, , \qquad f_{sd}^{hh'} = \sum (C_\alpha^{h'})^* C_\alpha^h \, f_\alpha \, , \tag{2.2}$$

respectively, such that the forward single diffractive cross section

$$\sum_{h' \neq h} \frac{d\sigma_{sd}}{dt}\Big|_{t=0} = \frac{1}{4\pi} \Big[\sum_{h'} |f_{sd}^{hh'}|^2 - |f_{el}^{hh}|^2 \Big] = \frac{\langle f_\alpha^2 \rangle - \langle f_\alpha \rangle^2}{4\pi} \tag{2.3}$$

is given by the dispersion of the eigenvalues distribution.

It was suggested in Ref. [11] that eigenstates of QCD interactions are color dipoles, such that any diffractive amplitude can be considered as a superposition of universal elastic dipole amplitudes. Such dipoles experience only elastic scattering and characterized only by transverse separation $\vec{r}$. The total hadron-proton cross section is then given by its eigenvalue, the universal dipole cross section

$$\sigma(\vec{r}) \equiv \int d^2b \, 2\mathrm{Im} f_{el}(\vec{b}, \vec{r}) \, , \tag{2.4}$$

as follows

$$\sigma_{tot}^{hp} = \sum |C_\alpha^h|^2 \sigma_\alpha = \int d^2r |\Psi_h(\vec{r})|^2 \sigma(\vec{r}) \equiv \langle \sigma(\vec{r}) \rangle \, , \tag{2.5}$$

where $\Psi_h(\vec{r})$ is the "hadron-to-dipole" transition wave function (incident parton momentum fractions are omitted). The dipole description of diffraction is based on the fact that dipoles of different transverse size $r_\perp$ interact with different cross sections $\sigma(r_\perp)$, leading to the single inelastic diffractive scattering with a cross section, which in the forward limit is given by [11],

$$\frac{\sigma_{sd}}{dp_\perp^2}\bigg|_{p_\perp=0} = \frac{\langle \sigma^2(\vec{r}) \rangle - \langle \sigma(\vec{r}) \rangle^2}{16\pi}, \tag{2.6}$$

where $p_\perp$ is the transverse momentum of the recoil proton, $\sigma(r)$ is the universal dipole-proton cross section, and operation $\langle \dots \rangle$ means averaging over the dipole separation. For

low and moderate energies, $\sigma(r)$ also depends on Bjorken variable x whereas in the high energy limit, the collision c.m. energy squared s is a more appropriate variable [24, 27]. The phenomenological dipole cross section fitted to data on inclusive DIS implicitly incorporates the effect of gluon bremsstrahlung. The latter is more important on a hard scale, this is why the small-distance dipole cross section rises faster with $1/x$.

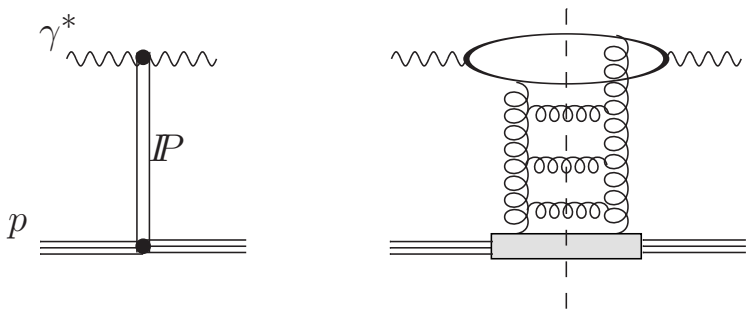

FIG. 1: The DIS cross section via phenomenological Pomeron exchange (left) and a perturbative QCD ladder (right). At small x the virtual photon fluctuates into a $q\bar{q}$ dipole and more complicated Fock states which then interact with the hadronic target.

Even for the simplest quark-anitiquark dipole configuration, a theoretical prediction of the partial dipole amplitude $f_{el}^{q\bar{q}}(\vec{b},\vec{r})$ and the dipole cross section $\sigma_{q\bar{q}}(\vec{r})$ from the first QCD principles is still a big challenge so these are rather fitted to data. The universality of the dipole scattering, however, enables us to fit known parameterizations to one set of known data (e.g. inclusive DIS) and use them for accurate predictions of other yet unknown observables (e.g. rapidity gap processes).

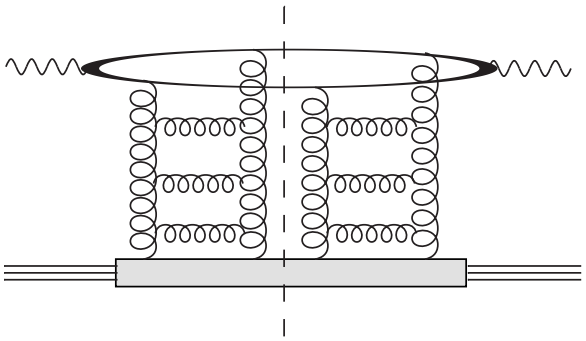

FIG. 2: The diffractive DIS cross section via double ladder exchange.

Indeed, at small Bjorken x in DIS the virtual photon exhibits partonic structure as shown in Fig. 1. The leading order configuration, the $q\bar{q}$ dipole, then elastically rescatters off the proton target p providing a phenomenological access to $\sigma_{q\bar{q}}(\vec{r},x)$. When it comes to diffractive DIS schematically represented in Fig. 2, the corresponding single diffractive cross section in the forward proton limit $t \to 0$ is given by the dipole cross section squared, i.e.

$$16\pi \left.\frac{d\sigma_{sd}^{\gamma^* p}(x,Q^2)}{dt}\right|_{t=0} = \int d^2r \int_0^1 d\alpha \, |\Psi_{\gamma^*}(\vec{r},\alpha,Q^2)| \, \sigma_{q\bar{q}}^2(\vec{r},x) \,, \tag{2.7}$$

where α is the light-cone momentum fraction of the virtual photon carried by the quark. Here, the dipole size $\vec{r}$ is regulated by the photon light-cone wave function Ψ_{γ^*} which can be found e.g. in Ref. [28]. The mean dipole size squared is inversely proportional to the quark energy squared

$$\langle r^2 \rangle \sim \frac{1}{\epsilon^2} = \frac{1}{Q^2\alpha(1-\alpha)+m_q^2}\,. \tag{2.8}$$

The dipole size is assumed to be preserved during scattering in the high energy limit.

Hard and soft hadronic fluctuations have small $\langle r^2\rangle \sim 1/Q^2$ (nearly symmetric $\alpha \gg m_q^2/Q^2$ configuration) and large $\langle r^2\rangle \sim 1/m_q^2$, $m_q \sim \Lambda_{\rm QCD}$ (aligned jet $\alpha \sim m_q^2/Q^2$ configuration) sizes, respectively. Remarkably enough, soft fluctuations play a dominant role in diffractive DIS in variance with inclusive DIS [10]. Although such soft fluctuations are very rare, their interactions with the target occur with a large cross section $\sigma \sim 1/m_q^2$ which largely compensate their small $\sim m_q^2/Q^2$ weights. On the other hand, abundant hard fluctuations with nearly symmetric small-size dipoles $\langle r^2\rangle \sim 1/Q^2$ have vanishing (as $1/Q^2$) cross section. It turns out that in inclusive DIS, both hard and soft contributions to the total cross section behave as $1/Q^2$ (semi-hard and semi-soft), while in diffractive DIS the soft fluctuations $\sim 1/m_q^2Q^2$ dominate over the hard ones $\sim 1/Q^4$. This also explains why the ratio σ_{sd}/σ_{inc} in DIS is nearly Q^2 independent as well as a higher-twist nature of the diffractive DIS.

The main ingredient of the dipole approach is the phenomenological dipole cross section, which is parameterized in the saturated form [27],

$$\sigma_{\bar{q}q}(r,x) = \sigma_0\big(1-e^{-r_p^2/R_0^2(x)}\big)\,, \tag{2.9}$$

and fitted to DIS data. Here, x is the Bjorken variable, $\sigma_0 = 23.03\,$mb and $R_0(x) = 0.4\,\text{fm}\times(x/x_0)^{0.144}$, where $x_0 = 0.003$. In pp collisions x is identified with gluon $x_2 = M^2/x_1 s \ll 1$ where M is the invariant mass of the produced system and s is the pp c.m. energy. This simplified parametrization (cf. Ref. [29]), appeared to be quite successful providing a reasonable description of HERA (DIS and DDIS) data.

In soft processes, however, the Bjorken variable x makes no sense, and gluon-target collision c.m. energy squared $\hat{s} = x_1 s$ (s is the pp c.m. energy) is a more appropriate variable, while the saturated form (2.9) should be retained [24]. The corresponding parameterisations for $\sigma_0 = \sigma_0(\hat{s})$ and $R_0 = R_0(\hat{s})$ read

$$R_0(\hat{s}) = 0.88\,\text{fm}\,(s_0/\hat{s})^{0.14}\,, \quad \sigma_0(\hat{s}) = \sigma_{tot}^{\pi p}(\hat{s})\Big(1+\frac{3R_0^2(\hat{s})}{8\langle r_{ch}^2\rangle_\pi}\Big)\,.$$

where the pion-proton total cross section is parametrized as [30] $\sigma_{tot}^{\pi p}(\hat{s}) = 23.6(\hat{s}/s_0)^{0.08}$ mb, $s_0 = 1000$ GeV^2, the mean pion radius squared is [31] $\langle r_{ch}^2\rangle_\pi = 0.44$ fm^2. An explicit analytic form of the x- and $\hat{s}$-dependent parameterisations for the elastic amplitude $f_{el}(\vec{b},\vec{r})$ accounting for an information about the dipole orientation w.r.t. the color background field (i.e. the angular dependence between $\vec{r}$ and $\vec{b}$) can be found in Refs. [32–34].

The ansatz (2.9) incorporate such important phenomenon as saturation at a soft scale since it levels off at $r \gg R_0$. Another important feature is vanishing of the cross section at small $r \to 0$ as $\sigma_{q\bar{q}} \propto r^2$ [11]. This is a general property called color transparency which reflects the fact that a point-like colorless object does not interact with external color fields. Finally, the quadratic r-dependence is an immediate consequence of gauge invariance and nonabeliance of interactions in QCD.

III. DIFFRACTIVE ABELIAN RADIATION: REGGE VS DIPOLE APPROACH

A. Diffractive factorisation

The cross section of the inclusive Drell-Yan (DY) is expressed via the dipole cross section in a way similar to DIS [35]

$$\frac{d\sigma_{\rm DY}(qp\to\gamma^* X)}{d\alpha dM^2}=\int d^2r|\Psi_{q\gamma^*}(\vec{r},\alpha)|^2\,\sigma_{q\bar{q}}(\alpha\vec{r})\,, \tag{3.1}$$

where α is the light-cone momentum fraction carried by the heavy photon off the parent quark. QCD factorisation relates inclusive DIS with DY, and similarity between these processes is the source of universality of the hadron PDFs.

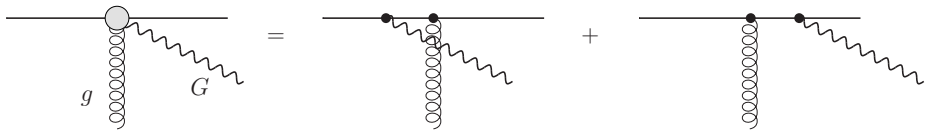

FIG. 3: Gauge boson radiation by a projectile quark in the target rest frame.

Now, consider the forward single diffractive Drell-Yan (DDY) and vector bosons production $G=Z,W^{\pm}$ in pp collisions which is characterized by a relatively small momentum transfer between the colliding protons. In particular, one of the protons, e.g. p_1, radiates a hard virtual gauge G^* boson with $k^2=M^2\gg m_p^2$ and hadronizes into a hadronic system X both moving in forward direction and separated by a large rapidity gap from the second proton p_2, which remains intact. In the DDY case,

$$p_1+p_2\to X+(gap)+p_2\,,\qquad X\equiv\gamma^*(l^+l^-)+Y\,. \tag{3.2}$$

Both the di-lepton and X, the debris of p_1, stay in the forward fragmentation region. In this case, the virtual photon is predominantly emitted by the valence quarks of the proton p_1.

In some of the previous studies [19, 36] of the single diffractive Drell-Yan reaction the analysis was made within the phenomenological Pomeron-Pomeron and γ-Pomeron fusion mechanisms using the Ingelman-Shlein approach [12] based on diffractive factorization. In analogy to the proven collinear factorisation [13] for inclusive processes, one assumes factorization of short and long distances in diffractive processes characterized by a hard scale. Besides one assumes that the soft part of the interaction, is carried out by Pomeron exchange, which is universal for different diffractive processes, i.e. Regge factorization is assumed as well. That could be true if the Pomeron were a true Regge pole, what is not supported by any known dynamical model. The above two assumptions lead to the following form of the diffractive DY cross section [36, 60] expresses in terms of the Pomeron PDFs $F_{\bar{q}/I\!P}$

$$\sigma_{sd}^{\rm DY}=G_{I\!P/p}\otimes F_{\bar{q}/I\!P}\otimes F_{q/p}\otimes\hat{\sigma}(q\bar{q}\to\bar{l}l)\,. \tag{3.3}$$

The diffractive factorisation leads to specific features of the differential DY cross sections similar to those in diffractive DIS process, e.g., a slow increase of the diffractive-to-inclusive DY cross sections ratio with c.m.s. energy $\sqrt{s}$, its practical independence on the hard scale, the invariant mass of the lepton pair squared, M^2 [19].

However, presence of spectator partons in hadronic collisions leads to a dramatic breakdown of diffractive factorization of short and long distances. On the contrary to inclusive processes, where spectator partons do not participate in the hard reactions in leading order, below we demonstrate that in diffraction the spectator partons do participate on a soft scale, i.e. their contribution is enhanced by Q^2/Λ^2. In particular, the spectator partons generate large absorptive corrections, usually called rapidity gap survival probability, which cause a strong suppression of the diffractive cross section compared with Eq. (3.3).

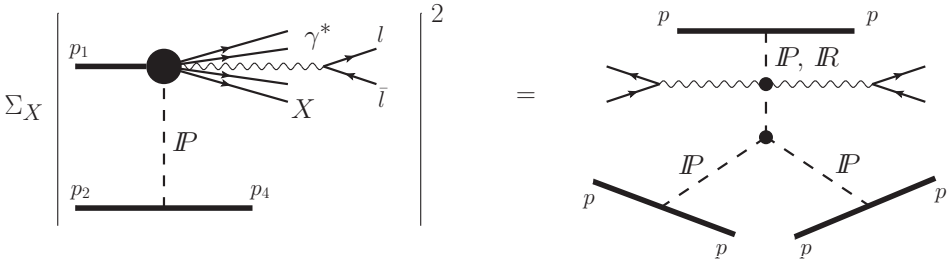

FIG. 4: The diffractive DY cross section summed over excitation channels at fixed effective mass M_X (left panel). The latter corresponds to the Mueller graph in Regge picture (right panel).

One can derive a Regge behavior of the diffractive cross section of heavy photon production in terms of the usual light-cone variables,

$$x_1 = \frac{p_\gamma^+}{p_1^+}; \qquad x_2 = \frac{p_\gamma^-}{p_2^-}, \tag{3.4}$$

so that $x_1 x_2 = (M^2 + k_T^2)/s$ and $x_1 - x_2 = x_F$, where M, k_T and x_F are the invariant mass, transverse momentum and Feynman variable of the heavy photon (di-lepton).

In the limit of small $x_1 \to 0$ and large $z_p \equiv p_4^+/p_2^+ \to 1$ the diffractive DY cross section is given by the Mueller graph shown in Fig. 4. In this case, the end-point behavior is dictated by the following general result

$$\frac{d\sigma}{dz_p dx_1 dt}\Big|_{t\to 0} \propto \frac{1}{(1-z_p)^{2\alpha_{I\!P}(t)-1} x_1^{\varepsilon}}\,, \tag{3.5}$$

where $\alpha_{I\!P}(t)$ is the Pomeron trajectory corresponding to the t-channel exchange, and ε is equal to 1 or 1/2 for the Pomeron $I\!P$ or Reggeon $I\!R$ exchange corresponding to γ^* emission from sea or valence quarks, respectively. Thus, the diffractive Abelian radiation process $pp \to (X \to G^* + Y)p$ at large Feynman $x_F \to 1$, or small

$$\xi = 1 - x_F = \frac{M_X^2}{s} \ll 1, \tag{3.6}$$

is described by triple Regge graphs in Fig. 5 where we also explicitly included radiation of a virtual gauge boson G^*. The Feynman graphs corresponding to the corresponding triple-Regge terms, are shown in Fig. 5 (second and third rows). The (ba) and (ca) diagrams illustrate the 3-Pomeron term, i.e.

$$\frac{d\sigma_{diff}^{I\!P I\!P I\!P}}{d\xi dt} \propto \xi^{-\alpha_{I\!P}(0)-2\alpha'_{I\!P}(t)}\,. \tag{3.7}$$

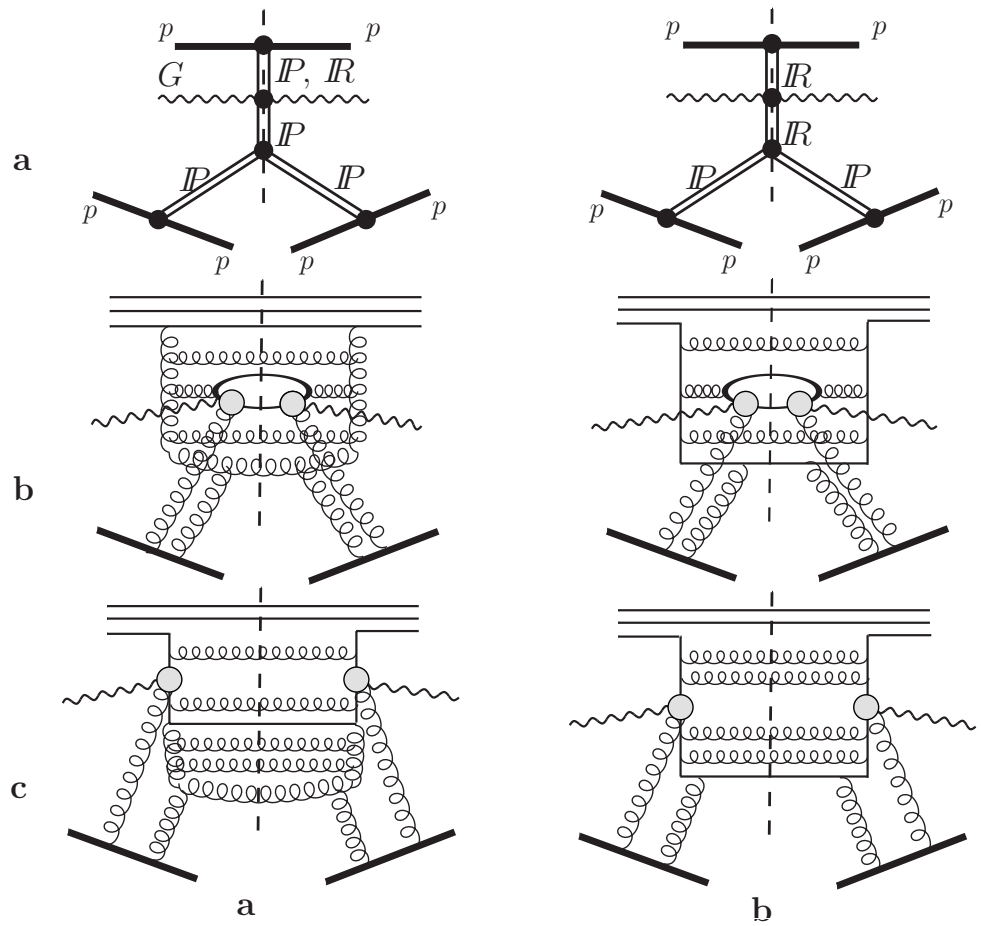

FIG. 5: The upper row contains the triple-Regge graphs for $pp \to (XG^*) + p$. A few key examples of diagrams for diffractive excitation of a large invariant mass are given by 2d and 3rd rows.

It is worth to mention that the smallness of the triple-Pomeron coupling is related to the known shortness of gluon correlation length. The amplitude $q + g \to q + G$ is given by open circles as in Fig. 3. So the 3-Pomeron term is interpreted as an excitation of the projectile proton due to the gluon radiation. The diffractive valence quark excitation is shown in Fig. 5, graphs (bb) and (cb) and contributes to

$$\frac{d\sigma_{diff}^{I\!P I\!P I\!R}}{d\xi dt} \propto \xi^{\alpha_{I\!R}(0)-\alpha_{I\!P}(0)-2\alpha'_{I\!P}(t)} . \tag{3.8}$$

B. Diffractive factorisation breaking in forward diffraction

As an alternative to the diffractive factorization based approach, the dipole description of the QCD diffraction, was presented in Refs. [11] (see also Ref. [37]). The color dipole description of inclusive Drell-Yan process was first introduced in Ref. [38] (see also Refs. [35, 39]) and treats the production of a heavy virtual photon via Bremsstrahlung mechanism rather than $\bar{q}q$ annihilation. The dipole approach applied to diffractive DY reaction in Refs. [6, 7] and later in diffractive vector boson production [8] has explictly demonstrated the diffractive factorisation breaking in diffractive Abelian radiation reactions.

It is worth emphasizing that the quark radiating the gauge boson cannot be a spectator, but must participate in the interaction. This is a straightforward consequence of the Good-Walker mechanism of diffraction [3]. According to this picture, diffraction vanishes if all Fock components of the hadron interact with the same elastic amplitudes. Then an unchanged Fock state composition emerges from the interaction, i.e. the outgoing hadron is the same as the incoming one, so the interaction is elastic.

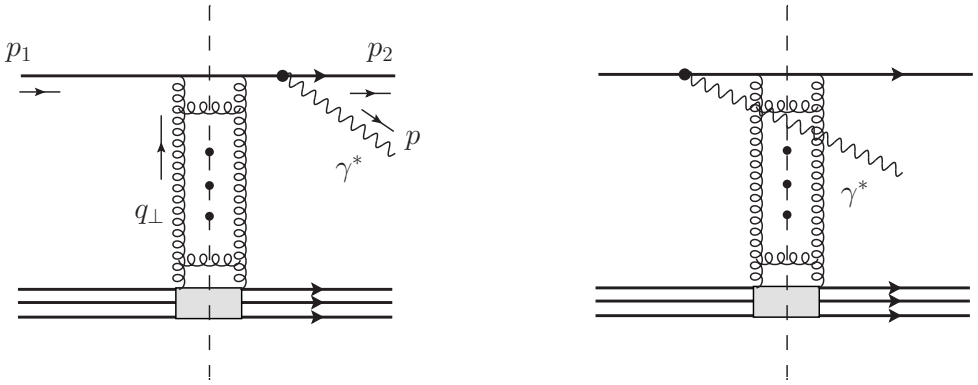

FIG. 6: Schematic illustration of the typical contributions and kinematics of the diffractive Drell-Yan process in the quark-target collision.

For illustration, consider diffractive photon radiation off a quark [24]. The relevant contributions and kinematics of the process are schematically presented in Fig. 6 where the Pomeron exchange is depicted as an effective two-gluon (BFKL) ladder. The corresponding framework has previously been used for diffractive gluon radiation and diffractive DIS processes in Refs. [24, 40, 41] and we adopt similar notations in what follows. Applying the generalized optical theorem in the high energy limit with a cut between the "screening" and "active" gluon as shown by dashed line in Fig. 6 we get,

$$\begin{aligned}\hat{A}_{SD} \;=\; & \frac{i}{2}\sum_{Y_8^*}\Big[\hat{A}^\dagger(q\gamma p\to q\{Y_8^*\})\hat{A}(qp\to q\{Y_8^*\}) \\ & +\;\hat{A}^\dagger(q\gamma p\to q\gamma\{Y_8^*\})\hat{A}(qp\to q\gamma\{Y_8^*\})\Big]\,, \end{aligned} \tag{3.9}$$

with summation going through all octet-changed intermediate states $\{Y_8^*\}$. In Eq. (3.9), the first and second terms correspond to the first and second diagrams in Fig. 6. Then we switch to impact parameter representation,

$$\hat{A}(\vec{b},\vec{r}) = \frac{1}{(2\pi)^4}\int d^2\vec{q}_\perp\, d^2\vec{\kappa}\;\hat{A}(\vec{q}_\perp,\vec{\kappa})\, e^{-i\vec{q}_\perp\cdot\vec{b}-i\vec{\kappa}\cdot\vec{r}}\,, \qquad \vec{\kappa}=\alpha\vec{p}_2-(1-\alpha)\vec{p}, \tag{3.10}$$

where $\vec{q}_\perp$, $\vec{p}_2$, $\vec{p}$ are the transverse momenta of the Pomeron, final quark and the radiated photon γ^*, α is the longitudinal momentum fraction of the photon taken off the parent quark p_1, and κ is the relative transverse momentum between the final quark and γ^*. Thus, the amplitude of the "screening" gluon exchange summed over projectile valence quarks

$j = 1, 2, 3$ reads

$$\hat{A}(qp \to q\{Y_8^*\}) = \sum_a \tau_a \langle f|\hat{\gamma}_a(\vec{b}_1)|i\rangle\,, \quad \hat{A}(q\gamma p \to q\gamma\{Y_8^*\}) = \sum_a \tau_a \langle f|\hat{\gamma}_a(\vec{b}_2)|i\rangle\,,$$
$$\hat{A}(qp \to q\gamma\{Y_8^*\}) = \hat{A}(q\gamma p \to q\gamma\{Y_8^*\}) = \sum_a \tau_a \Big[\langle f|\hat{\gamma}_a(\vec{b}_1)|i\rangle - \langle f|\hat{\gamma}_a(\vec{b}_2)|i\rangle\Big]\, \Psi_{q\to q\gamma}(\vec{r},\alpha)\,,$$

where $\vec{b}_1 \equiv \vec{b}$ and $b_2 \equiv \vec{b} - \alpha\vec{r}$ are the impact parameter of the quark before and after photon radiation, $\vec{r}$ is the transverse separation between the quark and the radiated photon, α is the momentum fraction taken by the photon, $\Psi_{q\to q\gamma}$ is the distribution function for the $q\gamma$ fluctuation of the quark, $\lambda_a = 2\tau_a$ are the Gell-Mann matrices from a gluon coupling to the quark, and the matrices $\hat{\gamma}_a$ are the operators in coordinate and color space for the target quarks,

$$\hat{\gamma}_a(\vec{R}) = \sum_i \tau_a^{(i)} \chi(\vec{R} - \vec{s}_i)\,, \qquad \chi(\vec{s}) \equiv \frac{1}{\pi}\int d^2q \frac{\alpha_s(q) e^{i\vec{q}\cdot\vec{s}}}{q^2 + \Lambda^2},$$

which depend on the effective gluon mass $\Lambda \sim 100$ MeV, and on the transverse distance between i-th valence quark in the target nucleon and its center of gravity, $\vec{s}_i$.

Combining these ingredients into the diffractive amplitude (3.9) one should average over color indices of the valence quarks and their relative coordinates in the target nucleon $|3q\rangle_1$. The color averaging results in,

$$\langle \tau_a^{(j)} \cdot \tau_{a'}^{(j')} \rangle_{|3q\rangle_1} = \begin{cases} \frac{1}{6}\delta_{aa'} & : j = j' \\ -\frac{1}{12}\delta_{aa'} & : j \neq j'. \end{cases}$$

Finally, averaging over quark relative coordinates $\vec{s}_i$ leads to

$$\langle i|\hat{\gamma}_a(\vec{b}_k)\hat{\gamma}_{a'}(\vec{b}_l)|i\rangle_{|3q\rangle_1} = \frac{3}{4}\delta_{aa'} S(\vec{b}_k, \vec{b}_l)\,,$$

where $S(\vec{b}_k, \vec{b}_l)$ is a scalar function, which can be expressed in terms of the quark-target scattering amplitude $\chi(\vec{r})$ and the proton wave function [24]. Then, the total amplitude,

$$\hat{A}(\vec{b}, \vec{r}) \propto S(\vec{b}, \vec{b}) - S(\vec{b} - \alpha\vec{r}, \vec{b} - \alpha\vec{r})\,.$$

After Fourier transform one notices that in the forward quark limit $q_\perp \to 0$ the amplitude for single diffractive photon or any Abelian radiation vanishes, $A(\vec{q}_\perp, \kappa)|_{q_\perp \to 0} = 0$, and

$$\frac{d\sigma_{sd}^{\rm DY}}{d\alpha dq_T^2}\Big|_{q_T=0} = 0\,,$$

in accordance with the Landau-Pomeranchuk principle. Indeed, in both Fock components of the quark $|q\rangle$ and $|q\gamma^*\rangle$, only the quark interacts, so these components interact equally and thus no diffraction is possible. One immediately concludes that the diffractive factorisation must be strongly broken.

The function $S(\vec{b}_k, \vec{b}_l)$ above is directly related to the $q\bar{q}$ dipole cross section as,

$$\sigma_{\bar{q}q}(\vec{r}_1 - \vec{r}_2) \equiv \int d^2b \Big[S(\vec{b} + \vec{r}_1, \vec{b} + \vec{r}_1) + S(\vec{b} + \vec{r}_2, \vec{b} + \vec{r}_2) - 2S(\vec{b} + \vec{r}_1, \vec{b} + \vec{r}_2)\Big]\,. \qquad (3.11)$$

Thus, following anological scheme one can obtain the diffractive amplitude of any diffractive process as a linear combination of the dipole cross sections for different dipole separations. As was anticipated, the diffractive amplitude represents the destructive interference effect from scattering of dipoles of slightly different sizes. Such an interference results in an interplay between hard and soft fluctuations in the diffractive pp amplitude, contributing to breakdown of diffractive factorisation.

When one considers diffractive DY off a finite-size object like a proton, in both Fock components, $|3q\rangle$ and $|3q\gamma^*\rangle$, only the quark hadron-scale dipoles interact. These dipoles are large due to soft intrinsic motion of quarks in the projectile proton wave function. The dipoles, however, have different sizes, since the recoil quark gets a shift in impact parameters. So the dipoles interact differently giving rise to forward diffraction. The contribution of a given projectile Fock state to the diffraction amplitude is given by the difference of elastic amplitudes for the Fock states including and excluding the gauge boson,

$$\Im f_{diff}^{(n)} = \Im f_{el}^{(n+G)} - \Im f_{el}^{(n)} \,, \tag{3.12}$$

where n is the total number of partons in the Fock state; $f_{el}^{(n+G)}$ and $f_{el}^{(n)}$ are the elastic scattering amplitudes for the whole n-parton ensemble, which either contains the gauge boson or does not, respectively. Although the gauge boson does not participate in the interaction, the impact parameter of the quark radiating the boson gets shifted, and this is the only reason why the difference Eq. (3.12) is not zero (see the next section). This also conveys that this quark must interact in order to retain the diffractive amplitude nonzero [6, 7]. For this reason in the graphs depicted in Fig. 5 the quark radiating G always takes part in the interaction with the target.

Notice that there is no one-to-one correspondence between diffraction in QCD and the triple-Regge phenomenology. In particular, there is no triple-Pomeron vertex localized in rapidity. The colorless "Pomeron" contains at least two t-channel gluons, which can couple to any pair of projectile partons. For instance in diffractive gluon radiation, which is the lowest order term in the triple-Pomeron graph, one of the t-channel gluons can couple to the radiated gluon, while another one couples to another parton at any rapidity, e.g. to a valence quark (see Fig. 3 in [24]). Apparently, such a contribution cannot be associated literally with either of the Regge graphs in Fig. 5. Nevertheless, this does not affect much the x_F- and energy dependencies provided by the triple-Regge graphs, because the gluon has spin one.

It is also worth mentioning that in Fig. 5 we presented only the lowest order graphs with two gluon exchange. The spectator partons in a multi-parton Fock component also can interact and contribute to the elastic amplitude of the whole parton ensemble. This gives rise to higher order terms, not shown explicitly in Fig. 5. They contribute to the diffractive amplitude Eq. (3.12) as a factor, which we define as the gap survival amplitude [8].

As was mentioned above the diffractive Abelian radiation off a dipole is non-vanishing in the forward domain which is different, for instance, from the $q \to q + \gamma^*$ case (see e.g. Refs. [6, 24]). Indeed, it is well-known that the off-diagonal diffraction is realised as long as different Fock states in the projectile hadron have different elastic interaction amplitudes [1–3, 5]. Due to the fluctuation $|q\rangle \to |qG\rangle$ the quark changes its position in the transverse plane by $\Delta\vec{r} = \alpha\vec{r}$ where $\vec{r}$ is the quark-boson transverse separation. Integrating over the impact parameter one realises that the Fock states corresponding to a single quark and a quark plus a boson interact with the same cross section such that a quark does not radiate at zeroth transverse momentum transfer. This happens under the assumption that the coherence

time with respect to the radiation is much larger than Δt scale between the subsequent interactions valid at forward rapidities. This is the main (model-independent) reason why diffractive production of G in the forward direction never realises (for more details, see Ref. [24, 42]).

The disappearance of both inelastic and diffractive forward Abelian radiation has a direct analogy in QED: if the electric charge gets no "kick", i.e. is not accelerated, no photon is radiated, provided that the radiation time considerably exceeds the duration time of interaction. This is dictated by the renown Landau-Pomeranchuk principle [43]: radiation depends on the strength of the accumulated kick, rather than on its structure, if the time scale of the kick is shorter than the radiation time. It is worth to notice that the non-Abelian QCD case is different: a quark can radiate gluons diffractively in the forward direction. This happens due to a possibility of interaction between the radiated gluon and the target. Such a process, in particular, becomes important in diffractive heavy flavor production [9].

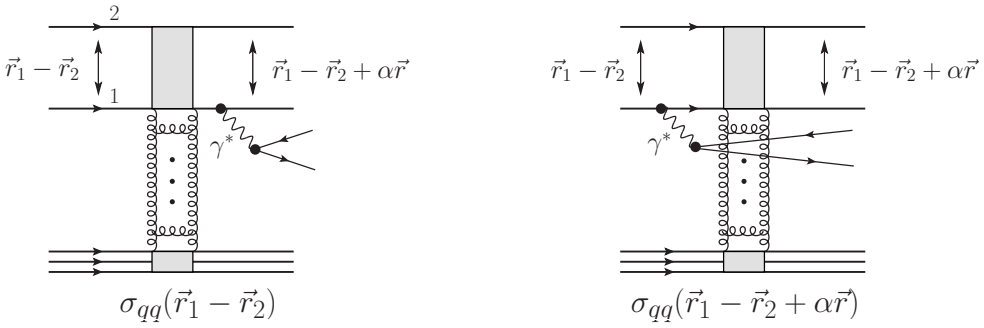

FIG. 7: Leading order contribution to the diffractive Drell-Yan in the dipole-target collision.

This is different for the boson radiation off a dipole Fig. 7. Such radiation induces a change in transverse separation between the dipole constituents after the scattering. Since different-size dipoles interact with the target with a different strength the diffractive radiation amplitude in this case is given by a difference [6]

$$M_{\bar{q}q}^{\rm diff} \propto \Psi(\alpha,\vec{r})\Big(2{\rm Im}\, f_{\rm el}(\vec{b},\vec{R}) - 2{\rm Im}\, f_{\rm el}(\vec{b},\vec{R}+\alpha\vec{r})\Big)\,, \tag{3.13}$$

where $\Psi_{q\to G^*q}$ is the light-cone (non-normalised) wave function of $q\to G^*q$ fluctuation corresponding to bremsstrahlung of virtual gauge bosons $G=\gamma,\,Z,\,W^\pm$ of mass M [8], $\vec{R}=\vec{r}_1-\vec{r}_2$ is the transverse size of the $q\bar{q}$ dipole, α is the momentum fraction of the gauge boson G taken off the parent quark q and $r\sim 1/M$ is the hard scale.

When applied to diffractive pp scattering the diffractive amplitude (3.13), thus, occurs to be sensitive to the large transverse separations between the projectile quarks in the incoming proton. Normally, transition to the hadron level is achieved by using the initial proton Ψ_i and remnant Ψ_f wave functions which encode information about distributions of consituents. The completeness relation reads

$$\begin{aligned}\sum_{fin}&\Psi_{fin}(\vec{r}_1,\vec{r}_2,\vec{r}_3;\{x_q^{1,2,\dots}\},\{x_g^{1,2,\dots}\})\Psi^*_{fin}(\vec{r}\,'_1,\vec{r}\,'_2,\vec{r}\,'_3;\{x'^{1,2,\dots}_q\},\{x'^{1,2,\dots}_g\})\\ &=\delta\big(\vec{r}_1-\vec{r}\,'_1\big)\delta(\vec{r}_2-\vec{r}\,'_2)\delta(\vec{r}_3-\vec{r}\,'_3)\prod_j\delta(x^j_{q/g}-x'^j_{q/g})\,.\end{aligned} \tag{3.14}$$

Here, $\vec{r}^{\,i}_{q/g}$, $x^i_{q/g}$ are the coordinates and fractions of the valence and sea partons, respectively.

Since gluons and sea quarks are mostly accumulated in a close vicinity of valence quarks (inside gluonic "spots"), to a reasonable accuracy the transverse positions of sea quarks and gluons can be identified with the coordinates of valence quarks. The valence part of the wave function is often taken to be a Gaussian distribution such that

$$\begin{aligned} |\Psi_{in}|^2 \;&=\; \frac{3a^2}{\pi^2} e^{-a(r_1^2+r_2^2+r_3^2)}\, \mathcal{R}\big(x_1, \{x_q^{1,2,\cdots}\}, \{x_g^{2,3,\cdots}\}\big) \\ &\times\; \delta(\vec{r}_1+\vec{r}_2+\vec{r}_3)\delta\Big(1-x_1-\sum_j x^j_{q/g}\Big)\,, \end{aligned} \tag{3.15}$$

where all the partons not participating in the hard interaction are summed up; x_1 is the photon fraction taken from the initial proton; $a=\langle r^2_{ch}\rangle^{-1}$ is the inverse proton mean charge radius squared; $\mathcal{R}$ is a collinear multi-parton distribution in the proton. Once the latter is integrated over all the partons not participating in the hard interaction, one gets a conventional collinear PDF $g(x_1,\mu^2)$ for gluons and $q(x_1,\mu^2)$ for a given quark flavor q. Since the diffractive pp cross section appears as a sum of diffractive excitations of the proton constituents, valence/sea quarks and gluons are incorporated as

$$\big|\Psi_{in}(\vec{r}_i,x_i)\big|^2 \propto \frac{1}{3}\left[\sum_q q(x)+\bar{q}(x)+\frac{81}{16}\,g(x)\right]\,, \tag{3.16}$$

after intergation over spectator impact parameters and momentum fractions with a proper color factor between quark and gluon PDFs. Note, only sea and valence quarks are excited by the photon radiation in the diffractive DY process which provide a direct access to the proton structure function in the soft limit of large x [35]

$$\sum_q Z_q^2[q(x)+\bar{q}(x)] = \frac{1}{x}\,F_2(x)\,.$$

For diffractive gluon radiation one should account for both quark and gluon excitations whose amplitudes, however, are calculated in different ways [24].

Due to the internal transverse motion of the projectile valence quarks inside the incoming proton, which corresponds to finite large transverse separations between them, the forward photon radiation does not vanish [6, 8]. These large distances are controlled by a non-perturbative (hadron) scale $\vec{R}$, such that the diffractive amplitude has the Good-Walker structure,

$$M^{\rm diff}_{\bar{q}q} \propto \sigma(\vec{R})-\sigma(\vec{R}-\alpha\vec{r}) \propto \vec{r}\cdot\vec{R}\,, \tag{3.17}$$

while the single diffractive-to-inclusive cross sections ratio behaves as

$$\frac{\sigma^{\rm DY}_{sd}}{\sigma^{\rm DY}_{incl}} \propto \frac{\exp(-2R^2/R_0^2(x_2))}{R_0^2(x_2)} \tag{3.18}$$

assuming the saturated GBW shape of the dipole cross section (2.9) where x_2 is defined in Eq. (3.4). Thus, the soft part of the interaction is not enhanced in Drell-Yan diffraction which is semi-hard/semi-soft like inclusive DIS. Linear dependence on the hard scale $r\sim$

$1/M \ll R_0(x_2)$ means that even at a hard scale the Abelian radiation is sensitive to the hadron size due to a dramatic breakdown of diffractive factorization [36]. It was firstly found in Refs. [44, 45] that factorization for diffractive Drell-Yan reaction fails due to the presence of spectator partons in the Pomeron. In Refs. [6–8] it was demonstrated that factorization in diffractive Abelian radiation is thus even more broken due to presence of spectator partons in the colliding hadrons as reflected in Eq. (3.17).

The effect of diffractive factorisation breaking manifests itself in specific features of observables like a significant damping of the cross section at high $\sqrt{s}$ compared to the inclusive production case as illustrated in Fig. 8. This is rather unusual, since a diffractive cross section, which is proportional to the dipole cross section squared, could be expected to rise with energy steeper than the total inclusive cross section, like it occurs in the diffractive DIS process. At the same time, the ratio of the DDY to DY cross sections was found in Ref. [6, 7] to rise with the hard scale, the photon virtuality M^2 also shown in Fig. 8. This is also in variance with diffraction in DIS, which is associated with the soft interactions and where the diffractive factorisation holds true [10].

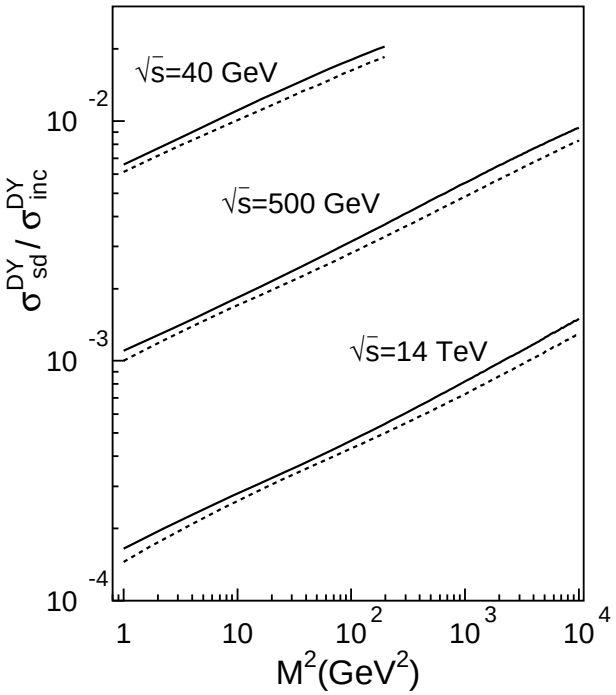

FIG. 8: The single diffractive-to-inclusive DY cross sections ratio as a function of the photon virtuality M^2 for $x_1 = 0.5$ (solid lines) and $x_1 = 0.9$ (dashed lines) and c.m.s. energies $\sqrt{s} =$ 40 GeV, 500 GeV and 14 TeV (from top to bottom) [6].

Such striking signatures of the diffractive factorisation breaking are due to an interplay of soft and hard interactions in the corresponding diffractive amplitude. Namely, large and small size projectile fluctuations contribute to the diffractive Abelian radiation process on the same footing providing the leading twist nature of the process, whereas diffractive DIS dominated by soft fluctuations only is of the higher twist [6, 7]. But this is not the only source of the factorisation breaking – another important source is the absorptive (or unitarity) corrections.

C. Gap survival amplitude

In the limit of unitarity saturation (the so-called black disk limit) the absorptive corrections can entirely terminate the large rapidity gap process. The situation close to this limit, in fact, happens in high energy (anti)proton-proton collisions such that unitarity is nearly saturated at small impact parameters [46, 47]. The unitarity corrections are typically parameterized by a suppression factor also known as the soft survival probability which significantly reduce the diffractive cross section. In hadronic collisions this probability is controlled by the soft spectator partons which are absent in the case of diffractive DIS causing the breakdown of diffractive factorisation.

It is well-known that the absorptive corrections affect differently the diagonal and off-diagonal terms in the hadronic current [5, 48], in opposite directions, leading to an additional source of the QCD factorisation breaking in processes with off-diagonal contributions only. Namely, the absorptive corrections enhance the diagonal terms at larger $\sqrt{s}$, whereas they strongly suppress the off-diagonal ones. In the diffractive DY process a new state, the heavy lepton pair, is produced, hence, the whole process is of entirely off-diagonal nature, whereas the diffractive DIS process contains both diagonal and off-diagonal contributions [5].

The amplitude Eq. (3.13) implicitly incorporates the absorptive effects thus does not requires a soft survival probability multiplier like traditionally imposed [8]. Consider a naive example when a dipole scatters elastically off a given potential. Then, the corresponding dipole partial amplitude emerges in the following eikonal form

$$\mathrm{Im}\, f_{el}(\vec{b},\vec{r}_1-\vec{r}_2)=1-\exp\Big(i\chi(\vec{r}_1)-i\chi(\vec{r}_2)\Big)\,,\qquad \chi(b)=-\int\limits_{-\infty}^{\infty}dz\,V(\vec{b},z)\,, \tag{3.19}$$

in terms of the potential $V(\vec{b},z)$. This amplitude is close to imaginary in the high-energy limit. A diffractive amplitude is then always proportional to the following difference

$$\mathrm{Im}\, f_{\rm el}(\vec{b},\vec{r}_1-\vec{r}_2+\alpha\vec{r})-\mathrm{Im}\, f_{\rm el}(\vec{b},\vec{r}_1-\vec{r}_2)\simeq\exp\Big(i\chi(\vec{r}_1)-i\chi(\vec{r}_2)\Big)\,\exp\Big(i\alpha\,\vec{r}\cdot\vec{\nabla}\chi(\vec{r}_1)\Big)\,, \tag{3.20}$$

where the first exponential factor provides the survival amplitude vanishing in the limit of the black disc as needed such that the diffractive amplitude Eq. (3.13) incorporates all absorptive corrections (gap survival amplitude), provided that the dipole cross section is adjusted to the data. While normally the survival factor is incorporated into the diffractive observables probabilistically, Eq. (3.13) treats more naturally quantum-mechanically.

The diffractive gluon radiation is know to be rather weak (the 3-Pomeron coupling is small). This phenomenological observation can be explained assuming that gluons in the proton are predominantly located inside small "gluonic spots" of size $r_0\sim 0.3\,\mathrm{fm}$ around the valence quarks (see e.g. Refs. [24, 49–51]). The smallness of gluonic dipole is an important nonperturbative phenomenon which may be connected e.g. to the small size of gluonic fluctuations in the instanton liquid model [50]. Therefore, a distance between a valence quark and a gluon in a vicinity of another quark can be safely approximated by the quark-quark separation.

Besides the soft gluons in the proton light-cone wave function, virtual gauge boson production triggers intensive gluon radiation such that there are many more spectator gluons in a vicinity of the quark which radiates the gauge boson. The separations of such gluons from the parent quark are controlled by the QCD DGLAP dynamics. In practice, one may

replace such a set of gluons by dipoles [52] whose transverse sizes r_d vary between $1/M_G$ and r_0 scales [53]. Then the mean dipole size is regulated by a relation

$$\langle r_d^2 \rangle = \frac{r_0^2}{\ln(r_0^2 M_G^2)}\,, \tag{3.21}$$

leading to $\langle r_d^2 \rangle \approx 0.01\,\mathrm{fm}^2$, which means that it is rather small and the corresponding dipole cross section $\sigma \simeq C(x)\,\langle r_d \rangle^2$, where $C(x) = \sigma_0/R_0^2(x)$ rises with energy, is suppressed. For $x = M_G^2/s$ and naive GBW parameterisation [27] we get $\sigma \approx 0.9\,\mathrm{mb}$ at the Tevatron energy. Each such small dipole brings up an extra suppression factor to the large rapidity gap survival amplitude given by

$$S_d(s) = 1 - \Im f_d(b, r_d)\,. \tag{3.22}$$

Here, the second term is small and thus is simplified to (for more details, see Ref. [54]),

$$\Im f_d(b, r_d) \approx \frac{\sigma_d}{4\pi B_d}\, e^{-b^2/2B_d}\,, \tag{3.23}$$

where B_d is the standard dipole-nucleon elastic slope $B_d \approx 6\,\mathrm{GeV}^{-2}$ measured earlier in diffractive ρ electro-production at HERA [55]. At the mean impact parameter given by $\langle b^2 \rangle = 2B_d$ and for the Tevatron energy $\sqrt{s} = 2\,\mathrm{TeV}$ we arrive at negligibly small value for the absorptive correction (3.23): $\Im f_d(0, r_d) \approx 0.01$.

On the other hard, the overall number of such dipoles increases with hardness of the process, which can amplify the magnitude of the absorptive effect. Generalising the gap survival amplitude to n_d projectile dipoles, we obtain

$$S_d^{(n_d)} = \left[1 - \Im f_d(b, r_d)\right]^{n_d}\,. \tag{3.24}$$

The DGLAP evolution formulated in impact parameter representation [53] enables to estimate the mean number of such dipoles can be estimated in the double-leading-log approximation

$$\langle n_d \rangle = \sqrt{\frac{12}{\beta_0} \ln\left(\frac{1}{\alpha_s(M_G^2)}\right) \ln\left((1 - x_F)\frac{s}{s_0}\right)}\,. \tag{3.25}$$

Here, the typical Bjorken x values of the radiated gluons is restricted by the diffractive mass as $x > s_0/M_X^2 = s_0/(1 - x_F)s$. In typical kinematics at the Tevatron collider, the mean number of such dipoles is roughly $\langle n_d \rangle \lesssim 6$. The amplitude of survival of a large rapidity gap is controlled by the largest dipoles in the projectile hadron only, such that the first exponential factor in Eq. (3.20) provides a sufficiently good approximation to the gap survival amplitude. The absorptive corrections (3.24) to the gap survival amplitude are proven to be rather weak and do not exceed 5% (or 10% in the survival probability factor) which is small compared to an overall theoretical uncertainty. For the pioneering work on hard rescattering corrections to the gap survival factor see Ref. [56].

The popular quasi-eikonal model for the so-called "enhanced" probability $\hat{S}_{enh}$ (see e.g. Refs. [22, 57]), frequently used to describe the factorisation breaking in diffractive processes, is not well justified in higher orders, whereas the color dipole approach considered here, correctly includes all diffraction excitations to all orders [5]. Such effects are included into the phenomenological parameterizations for the partial elastic dipole amplitude fitted to data. This allows to predict the diffractive gauge bosons production cross sections in terms

of a single parameterization for the universal dipole cross section (or, equivalently, the elastic dipole amplitude) known independently from the soft hadron scattering data.

For more details on derivations of diffractive gauge boson production amplitudes and cross sections see Refs. [7, 8]. Now we turn to a discussion of numerical results for the most important observables.

IV. SINGLE DIFFRACTIVE GAUGE BOSONS PRODUCTION

In Ref. [8] the dipole framework has been used in analysis of diffractive gauge bosons production, and here we briefly overview these results. The corresponding observables for Z^0, γ^*, $W^\pm$ production ($\sqrt{s} = 14$ TeV) such as $d\sigma_{sd}/dM^2$ and $d\sigma_{sd}/dx_1$ are shown in Fig. 9 at left and right panels, respectively. The M^2 distributions correspond to the forward rapidities, i.e. $0.3 < x_1 < 1$ and the interval $5 < M^2 < 10^5$ GeV^2 is concerned.

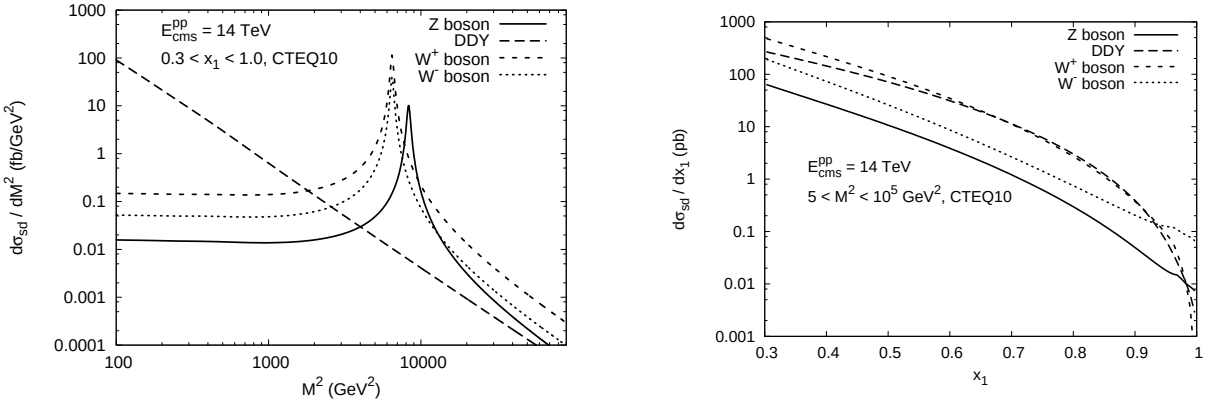

FIG. 9: The cross section for diffractive boson production as a function of M^2 (left) and fraction x_1 (right) at the energy of LHC.

In the region corresponding to the resonant Z^0, $W^\pm$ bosons production, the M^2 distributions exceed the diffractive γ^* component. The latter is relevant for low masses only. As for the x_1-distributions of W^+ and γ^* components, these are relatively close to each other, whereas the W^-, Z-boson components are smaller. A precision measurement of diffractive $W^\pm$ distributions and their differences may enable further constraining of the quark PDFs at large quark momentum fractions x_1/α.

Another phenomenologically interesting observable is the lepton-pair $q_\perp$ differential distribution at the LHC shown in Fig. 10 (left). The $W^\pm$ charge asymmetry is particularly dependent on the u, d PDFs difference at large x. It is given by

$$A_W \equiv \frac{d\sigma_{sd}^{W^+}/dx_1 - d\sigma_{sd}^{W^-}/dx_1}{d\sigma_{sd}^{W^+}/dx_1 + d\sigma_{sd}^{W^-}/dx_1}\,. \tag{4.1}$$

and is shown in Fig. 10 (right panel). The quantity does not depend on both the invariant mass/energy.

Similarly to diffractive DY discussed above, an important feature of the SD-to-inclusive ratio as a function of M^2, x_1

$$R = \frac{d\sigma_{sd}/dx_1 dM^2}{d\sigma_{incl}/dx_1 dM^2}\,, \tag{4.2}$$

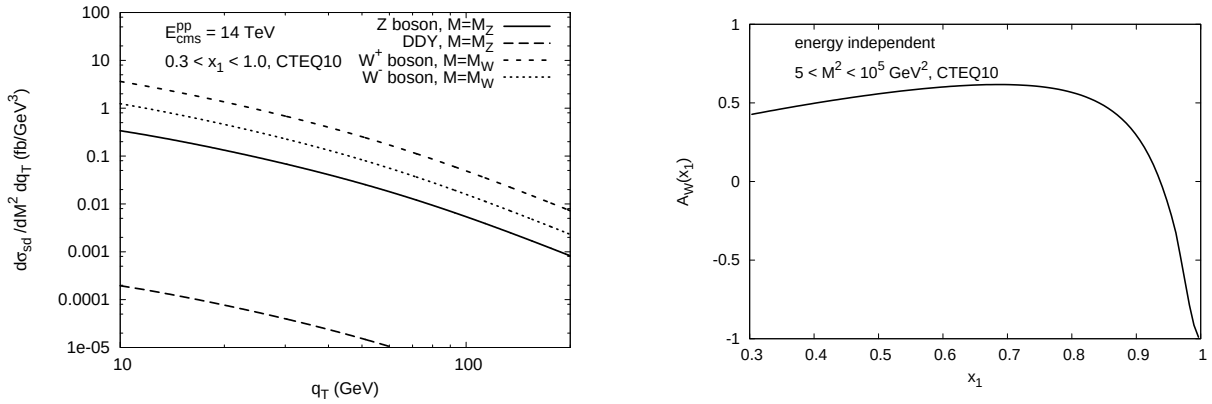

FIG. 10: The lepton pair transverse momentum $q_\perp$ distribution the diffractive cross section at the LHC $\sqrt{s} = 14$ TeV (left panel) and the charge asymmetry in the SD $W^\pm$ cross sections at fixed $M^2 = M_W^2$ (right panel).

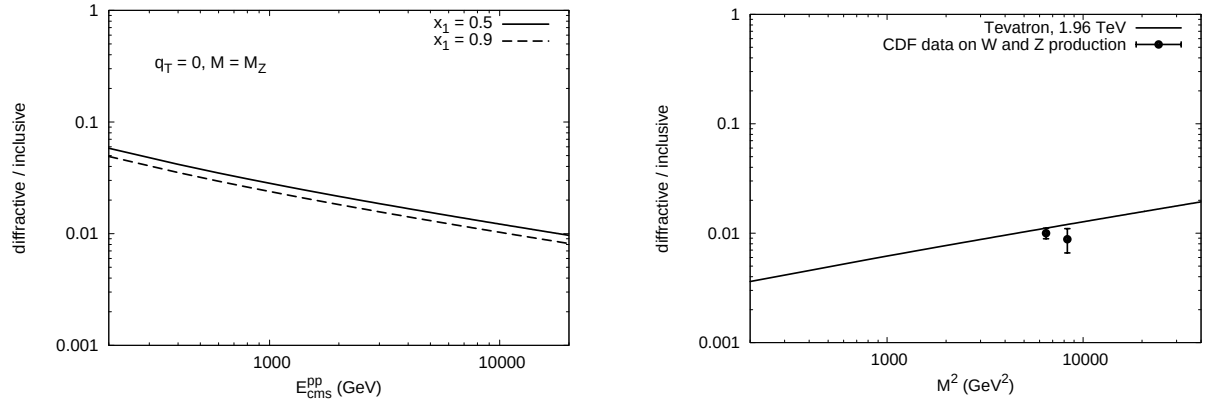

FIG. 11: The SD-to-incl. ratio w.r.t. the collision energy $\sqrt{s}$ (left) as well as M^2 at Tevatron (right).

which exhibits an non-typical energy as well as hard scale dependence (see Fig. 11) compared to the conventional diffractive QCD factorisation based predictions [19, 20]. In analogy to DDY case, this ratio behaves w.r.t. the energy and the hard scale in opposite way to what is expected from diffractive factorisation. The ratio does not depend on the properties of the radiated gauge boson and PDFs while it is sensitive to the partial dipole amplitude structure only efficiently probing the QCD mechanism of diffraction. Thus, the diffractive gauge boson observables in the di-lepton channel which enhanced compared to DDY around the Z^0 and $W^\pm$ resonances provides crucial details on the soft/hard fluctuations and their interplay in QCD.

V. DIFFRACTIVE NON-ABELIAN RADIATION

As we have seen in the discussion above, diffractive DY is one of the most important examples of leading-twist processes, where simultaneously large and small size projectile fluctuations are at work. It turns out that the participation of soft spectator partons in the

interaction with the gluonic ladder is crucial and results in a leading twist effect. What are other examples of the leading twist behavior in diffraction?

A. Leading-twist diffractive heavy flavor production

One might naively think that the Abelian (or DIS) mechanism of heavy flavor production $\gamma^* \to Q\bar{Q}$ is of the leading twist as well since it behaves as $\sim 1/Q^2$. However, in the limit $m_Q^2 \gg Q^2$ the corresponding cross section $\sigma_{sd} \propto 1/m_Q^4$ i.e. behaves as a higher twist process. One has to radiate at least one gluon off the $Q\bar{Q}$ pair for this process to become the leading twist one, e.g. $\sigma_{sd}(\gamma^* \to Q\bar{Q}g) \propto 1/m_Q^2$, since the mean transverse separation between G and small $Q\bar{Q}$ dipole is typically large although formally such a process is of the higher perturbative QCD order in α_s.

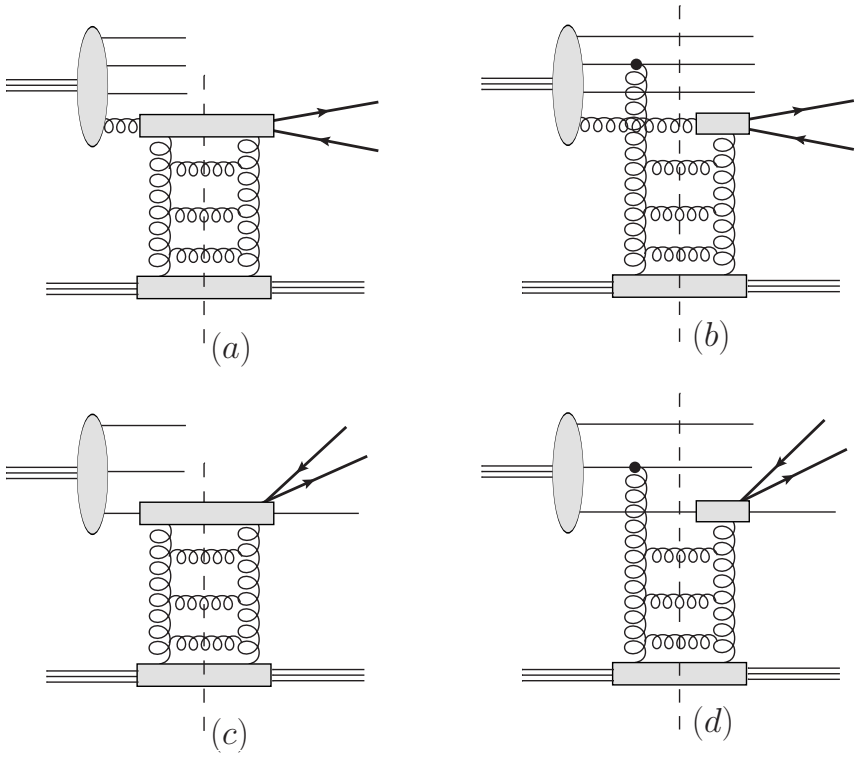

FIG. 12: Leading order contributions to single diffractive heavy flavor production in gluon-proton (a,b) and quark-proton (c,d) scattering subprocesses in pp collisions. Diagrams (b,d) emerge due to the presence of soft spectator partons in the proton wave function (the screening gluon couples to every spectator parton besides the active one). Grey effective vertices account for all possible couplings of the incident partons.

Consider now the non-Abelian mechanism for diffractive hadroproduction of heavy quarks via $g^* \to Q\bar{Q}$ hard subprocess. Production of heavy quarks at large $x_F \to 1$ is a longstanding controversial issue even in inclusive processes. On one hand, QCD factorisation approach predicts vanishingly small yields of heavy flavor due to steeply falling gluon density as $\sim (1-x_F)^5$ at large x_F. On the other hand, the end-point behavior is controlled by the universal Regge asymptotics $d\sigma/dx_F(x_F \to 1) \propto (1-x_F)^{1-2\alpha_R(t)}$ in terms of the Regge

trajectory of the t-channel exchange $\alpha_R(t)$. Apparently, the Regge and QCd factorisation approaches contradict each other. The same problem emerges in the DY process at large x_F as is seen in data [58] which means that in the considering kinematics the conventional QCD factorisation does not apply [59]. At the same time, the observation of an excess of diffractive production of heavy quarks at large $x_F \to 1$ compared to conventional expectation may provide a good evidence for intrinsic heavy flavors if the latter is reliably known. Calculations assuming that diffractive factorisation holds for hard diffraction [12, 60] may not be used for quantifying the effect from intrinsic heavy flavor. Instead, the dipole framework has been employed to this process for the first time in Ref. [9]. Here we briefly overview the basic theory aspects concerning primarily heavy quarks produced in the projectile fragmentation region (for inclusive $Q\bar{Q}$ production at mid rapidites in the dipole framework, see Ref. [61]).

Typical contributions to the single diffractive $Q\bar{Q}$ production rate are summarized in Fig. 12. Diagrams (a) and (b) correspond to the leading order gluon splitting into $Q\bar{Q}$ contributions in the color field of the target proton (diffractive gluon excitation). The latter gluon as a component of the projectile proton wave function can be treated as real (via collinear gluon PDF) or virtual (via unintegrated gluon PDF). Due to hard scale m_Q the diagram (a) with Pomeron coupling to a small-size $gQ\bar{Q}$ system is of the higher twist due to color transparency and is therefore suppressed. Diagram (b) involves two scales – the soft hadronic one $\sim \Lambda_{\rm QCD}$ associated with large transverse separations between a gluon and constituent valence quarks, and the hard one $\sim m_Q$ associated with small $Q\bar{Q}$ dipole. An interplay between these two scales similar to that in DDY emerges as the leading twist effect; thus, diagram (b) is important. Possible higher order terms with an extra gluon radiation contributing to the leading twist diffractive heavy flavor production were disscussed in detail in Ref. [9].

Diagrams (c) and (d) account for $Q\bar{Q}$ production via diffractive quark excitation. Just as in leading twist diffraction in DIS $\gamma^* \to Q\bar{Q}g$, these processes are associated with two characteristic transverse separations, a small one, $\sim 1/m_Q$, between the $\bar{Q}$ and Q, and a large one, either $\sim 1/m_q$ between q and $Q\bar{Q}$ (diagram (c)) or $1/\Lambda_{\rm QCD}$ between another constituent valence quark and $Q\bar{Q}$ (diagram (d)). While all the terms contributing to (d) are of the leading twist (see Ref. [9]), only a special subset of diagrams (c) are of the leading twist. Indeed, the hard subprocess $q + g \to (Q\bar{Q}) + q$ is characretized by five distinct topologies illustrated in Fig. 13, and similar graphs are for gluon-proton scattering with subprocess $g + g \to (Q\bar{Q}) + g$.

These graphs can be grouped into two amplitudes attributed to bremsstrahlung (BR) and production (PR) mechanisms, which do, or do not involve the projectile light quarks or gluons, respectively (for more details, see Fig. 2 and Appendix A in Ref. [9]). The BR mechanism includes the same graphs as radiation of a gluon (see Refs. [40, 62]), i.e. interaction with the source parton before and after radiation, and interaction with the radiated gluon. The PR mechanism, responsible for the transition $g \to \bar{Q}Q$, includes the interactions with the gluon and the produced $\bar{Q}Q$ (also known as gluon-gluon fusion $gg \to Q\bar{Q}$ mechanism). The total amplitude is

$$M_{q,g} = M_{q,g}^{\rm BR} + M_{q,g}^{\rm PR}\,, \tag{5.1}$$

where subscripts q, g denote contributions with hard gluon radiation by the projectile valence or sea quarks and gluons, respectively. Such grouping is performed separately for transversely and longitudinally polarised gluons as described in Ref. [9]). One of the reasons for this grouping is that each of these two combinations is gauge invariant and can be expressed in terms of three-body dipole cross sections, $\sigma_{g\bar{q}q}$ and $\sigma_{g\bar{Q}Q}$ respectively.

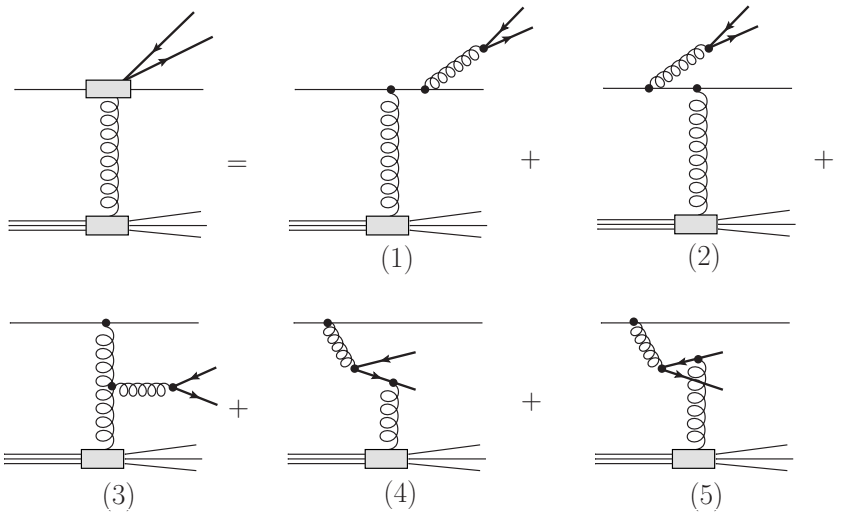

FIG. 13: Five different topologies contributing to inclusive $Q\bar{Q}$ production in quark-proton scattering. These can be split into two gauge-invariant subsets of amplitudes as described in the text.

Another physical reason for such a separation is different scale dependence of the BR and PR components. Introducing the transverse separations $\vec{r}$, $\vec{r}_1$ and $\vec{r}_2$ within the $\bar{Q}Q$, $q\bar{Q}$ and qQ pairs, respectively, the three body dipole cross sections can be expressed via two scales: the distance between the final light quark (or gluon) and the center of gravity of the $Q\bar{Q}$ pair, $\vec{\rho} = \vec{r} - \beta\vec{r}_1 - (1-\beta)\vec{r}_2$ (β is the heavy quark momentum fraction taken from the parent gluon which takes fraction α of the parent parton), and the $Q\bar{Q}$ transverse separation, $\vec{s} = \vec{r}_1 - \vec{r}_2$. The corresponding distribution amplitudes of $Q\bar{Q}$ production in diffractive quark/gluon scattering off proton

$$A_{\rm BR} \propto \Phi_{\rm BR}(\vec{\rho},\vec{s})\Sigma_1(\vec{\rho},\vec{s})\,, \qquad A_{\rm PR} \propto \Phi_{\rm PR}(\vec{\rho},\vec{s})\Sigma_2(\vec{\rho},\vec{s})\,, \tag{5.2}$$

are given in terms of the effective dipole cross sections for a colorless $g\bar{q}q$ and $g\bar{Q}Q$ systems, and rather complicated wave functions Φ of subsequent gluon radiation and then its splitting into $\bar{Q}Q$ pair in both cases. In the case of bremsstrahlung, both mean separations are controlled by the hard scale such that

$$A_{\rm BR} \sim \langle\rho^2\rangle \sim \langle s^2\rangle \sim \frac{1}{m_Q^2}\,,$$

thus, the corresponding contribution is a higher twist effect and thus suppressed (note, in the case of forward Abelian radiation this contribution is equal to zero). On the contrary, in the production mechanism only the $\bar{Q}Q$ separation is small, $\langle s^2\rangle \sim 1/m_Q^2$, the second scale appears to be soft, $\langle\rho^2\rangle \sim 1/m_q^2$, leading to the leading twist behavior

$$A_{\rm PR} \sim \vec{s}\cdot\vec{\rho}$$

in analogy to diffractive DY process. This is a rather nontrivial fact, since in the case of the DY reaction such a property is due to the Abelian nature of the radiated particle while here we consider a non-Abelian radiation. The bremsstrahlung-production interference terms are of the higher twist and thus are safely omitted.

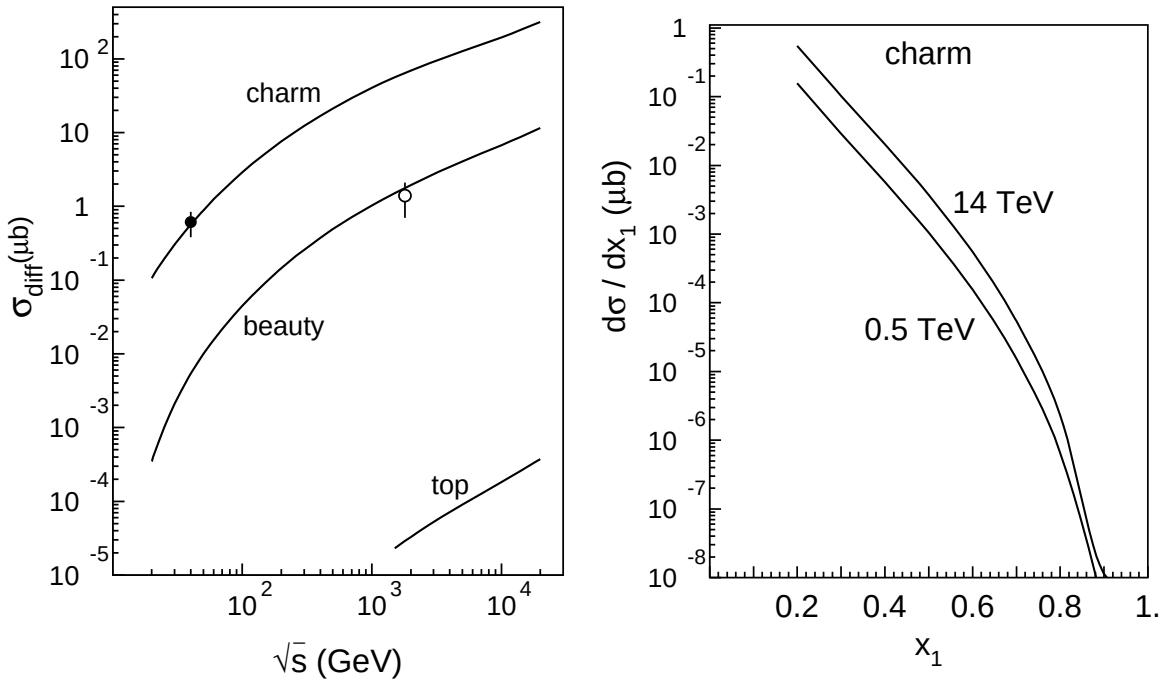

FIG. 14: The total cross section of diffractive $c\bar{c}$, $b\bar{b}$ and $t\bar{t}$ pairs production as function of energy in comparison with experimental data from E690 [63] and CDF [64] experiments (left panel) and the differential cross section as function of fraction x_1 of the initial proton momentum carried by the charm quark (right panel) [9].

The situation with scale dependence in the case of $\bar{Q}Q$ production in diffractive pp scattering is somewhat similar to diffractive quark-proton scattering discussed above but technically more involved due to extra terms (b) and (d) in Fig. 12 and color averaging over the projectile proton wave function. Although bremsstrahlung terms from diagrams (b), (d) are formally of the leading twist due to interactions with distant spectator partons, numerically they are always tiny due to denominator suppression by a large $\bar{Q}Q$ mass. Thus, the leading twist production terms from (b), (c), and (d) sets are relevant whereas the set (a) does not contain production terms and is a higher twist effect. Thus, like in diffractive Drell-Yan in the considering process the leading twist effect, at least, partly emerges due to intrinsic transverse motion of constituent quarks in the incoming proton. However, due to a non-Abelian nature of this process extra leading-twist terms production from the "production" mechanism, which are independent of the structure of the hadronic wave function, become important. Diffractive production cross sections of charm, beauty and top quark pairs, $p + p \to Q\bar{Q}X + p$, as functions of c.m.s. pp energy are shown in Fig. 14. The experimental data points available from E690 [63] and CDF [64] experiments have been compared with theoretical predictions evaluated with corresponding phase space constraints (for more details, see Ref. [9]).

B. Single diffractive Higgsstrahlung

Typically large Standard Model (SM) backgrounds and theoretical uncertainties due to higher order effects strongly limit the potential of inclusive Higgs boson production for

spotting likely small but yet possible New Physics effects. Some of the SM extensions predict certain distortions in Higgs boson Yukawa couplings such that the precision multi-channel measurements of the Higgs-heavy quarks couplings becomes a crutial test of the SM structure. As a very promising but challenging channel, the exclusive and diffractive Higgs production processes (involving rapidity gaps) offer new possibilities to constrain the backgrounds, and open up more opportunities for New Physics searches (see e.g. Refs. [65–72]).

The QCD-initiated gluon-gluon fusion $gg \to H$ mechanism via a heavy quark loop is one of the dominant and most studied Higgs bosons production modes in inclusive pp scattering which has led to its discovery at the LHC (for more information on Higgs physics highlights, see e.g. Refs. [73–78] and references therein). The same mechanism is expected to provide an important Higgs production mode in single diffractive pp scattering as well as in central exclusive Higgs boson production [65, 66, 69]. The forward inclusive and diffractive Higgsstrahlung off intrinsic heavy flavor at $x_F \to 1$ has previously been studied in Refs. [79, 80], respectively.

Very recently, a new single diffractive production mode of the Higgs boson in association with a heavy quark pair $\bar{Q}Q$, namely $pp \to X + Q\bar{Q}H + p$, at large x_F where conventional factorisation-based approaches are expected to fail has been studied in Ref. [21]. The latter process is an important background for diffractive Higgs boson hadroproduction off intrinsic heavy flavor. Here, we provide a short overview of this process which is analogical to forward diffractive $\bar{Q}Q$ production discussed above.

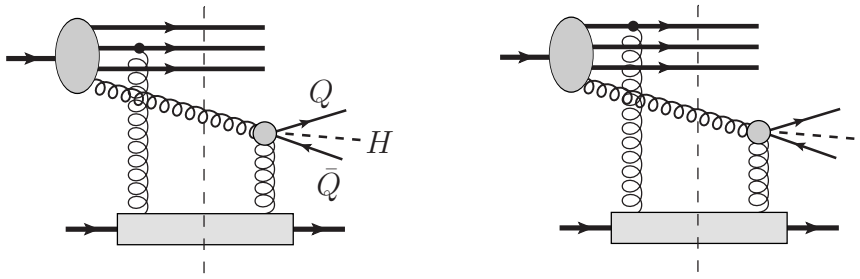

FIG. 15: Dominant gluon-initiated contributions to the single diffractive $\bar{Q}Q + H$ production [21].

For a reasonably accurate estimate one retains only the dominant gluon-initiated leading twist terms illustrated in Fig. 15 where the "active" gluon is coupled to the hard $Q\bar{Q} + H$ system, while the soft "screening" gluon couples to a spectator parton at a large impact distance. The latter are illustrated by tree-level diagrams with Higgs boson radiation off a heavy quark or Higgsstrahlung. In practice, however, one does not calculate the Feynman graphs explicitly in Fig. 15. Instead one should adopt the generalized optical theorem within the Good-Walker approach to diffraction [3] such that a diffractive scattering amplitude turns out to be proportional to a difference between elastic scatterings of different Fock states [21]. The contributions where both "active" and "screening" gluons couple to partons at small relative distances are the higher twist ones and thus are strongly suppressed by extra powers of the hard scale (see e.g. Refs. [9]). This becomes obvious in the colour dipole framework due to colour transparency [11] making the medium more transparent for smaller dipoles.

The hard scales which control the diffractive Higgsstrahlung process are, $\langle r^2 \rangle \sim 1/m_Q^2$ and $\langle \rho^2 \rangle \sim 1/\tau^2$, where $\tau^2 = M_H^2 + \alpha_3 M_{Q\bar{Q}}^2$ in terms of the Higgs boson mass, M_H, and the $Q\bar{Q}$ pair invariant mass, $M_{Q\bar{Q}}$. Another length scale here is the distance between ith and

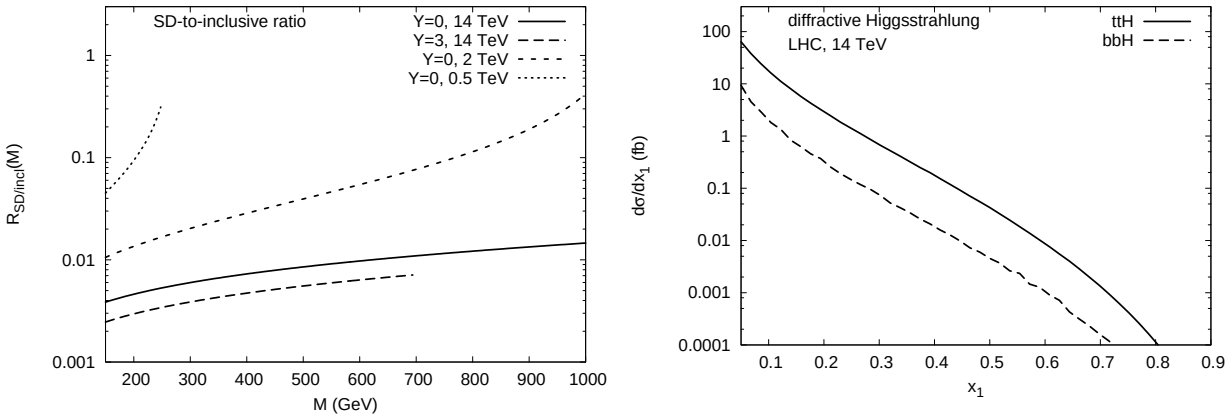

FIG. 16: The SD-to-inclusive ratio $R(M)$ as a function of $\bar{Q}QH$ invariant mass M for different c.m. energies $\sqrt{s} = 0.5, 2, 14$ TeV (left panel) and the differential cross section $d\sigma/dx_1$ of the SD Higgsstrahlung off $t\bar{t}$ and $b\bar{b}$ pairs for $\sqrt{s} = 14$ TeV (right panel) [21].

jth projectile partons, $\langle r_{ij}^2 \rangle \sim \langle R \rangle^2$, is soft for light valence/sea quarks in the proton wave function. Before the hard gluon splits into $\bar{Q}QH$ system it undergoes multiple splittings $g \to gg$ populating the projectile fragmentation domain with gluon radiation with momenta below the hard scale of the process $p_\perp^{rad} < M_{\bar{Q}QH}$. The latter should be accounted for via a gluon PDF evolution.

The SD-to-inclusive ratio of the cross sections for different c.m. energies $\sqrt{s} = 0.5, 7, 14$ TeV and for two distinct rapidities $Y = 0$ and 3 as functions of $\bar{Q}QH$ invariant mass M are shown in Fig. 16 (left). The ratio is similar to that for heavy quark production [9] and thus in good agreement with experimental data from the Tevatron. Note, this ratio has falling energy- and rising M-dependence, where M is the invariant mass of the produced $\bar{Q}QH$ system. This is similar to what was found for diffractive Drell-Yan process [7, 8] and has the same origin, namely, breakdown of QCD factorisation and the saturated form of the dipole cross section.

The differential cross sections of single diffractive $b\bar{b}$ and $t\bar{t}$ production in association with the Higgs boson are shown in Fig. 16 (right) as functions of x_1 variable at the LHC energy $\sqrt{s} = 14$ TeV implied that the Higgs boson transverse momentum is large, i.e. $\kappa \gtrsim m_H$. In this case the asymptotic dipole formula based upon the collinear projectile gluon PDF (3.16) and the first (quadratic) term in the dipole cross section is a good approximation and reproduces the exact $k_\perp$-factorisation result for the inclusive Higgsstrahlung transverse momentum distribution in both the shape and normalisation (for more details, see Ref. [21]). The contribution of diffractive gluon excitations to the Higgsstrahlung dominates the total Higgsstrahlung cross section due a large yield from central rapidities. Besides, the SD Higgsstrahlung off top quarks is larger than that from the bottom while shapes of the x_1 distributions are similar. Additional radiation of the Higgs boson enhances the contribution of heavy quarks and thus compensates the smallness of their diffractive production modes.

Analogically to other diffractive bremsstrahlung processes discussed in previous sections, breakdown of QCD factorisation leads to a flatter hard scale dependence of the cross section. This is a result of leading twist behaviour which have been discussed above and which has been confirmed by the comparison of data on diffractive production of charm and beauty [9].

VI. SUMMARY

In this short review, we have discussed major properties and basic dynamics of single diffractive processes of γ^*, Z^0 and $W^\pm$ bosons production processes at the LHC, as well as leading twist heavy flavor hadroproduction at large Feynman x_F and diffractive Higgsstrahlung off heavy quarks. We outlined the manifestations of diffractive factorisation breaking in these single diffractive reactions within the framework of color dipole description, which is suitable for studies of the interplay between soft and hard fluctuations. The latter reliably determine diffractive hadroproduction in the projectile fragmentation region.

The first, rather obvious source for violation of diffractive factorisation, is related to the absorptive corrections (called sometimes survival probability of large rapidity gaps). The absorptive corrections affect differently the diagonal and off-diagonal diffractive amplitudes [5, 48], leading to a breakdown of diffractive QCD factorisation in hard diffractive processes, like diffractive radiation of heavy Abelian particles and heavy flavors. The dipole approach enables to account for the absorptive corrections automatically at the amplitude level.

The second, more sophisticated reason for diffractive factorisation breaking, is specific for Abelian radiation, namely, a quark cannot radiate in the forward direction (zero momentum transfer), where diffractive cross sections usually have a maximum. Forward diffraction becomes possible due to intrinsic transverse motion of quarks inside the proton, although the magnitude of the forward cross section remains very small [6, 7]. A much larger contribution to Abelian radiation in the forward direction in pp collisions comes from interaction with the spectator partons in the proton. Such a hard-soft interplay is specific for the considered processes in variance to the DDIS involving no co-moving spectator partons.

These mechanisms of diffractive factorisation breaking lead to rather unusual features of the leading-twist diffractive Abelian radiation w.r.t. its hard scale and energy dependence.

The outlined sources of factorisation breaking are also presented in diffractive radiation of non-Abelian particles. Interactions of the radiated gluon makes it possible to be radiated even at zero momentum transfer. These processes have been quantitatively analysed in such important channels as diffractive heavy flavor production and Higgsstrahlung in the projectile fragmentation region. Further studies of these effects, both experimentally and theoretically, are of major importance for upcoming LHC measurements.

Acknowledgments

This study was partially supported by Fondecyt (Chile) grants 1120920, 1130543 and 1130549, and by ECOS-Conicyt grant No. C12E04. R. P. was partially supported by Swedish Research Council Grant No. 2013-4287.

[1] R. J. Glauber, Phys. Rev. 100, 242 (1955).

[2] E. Feinberg and I. Ya. Pomeranchuk, Nuovo. Cimento. Suppl. 3 (1956) 652.

[3] M. L. Good and W. D. Walker, Phys. Rev. 120 (1960) 1857.

[4] A. B. Kaidalov, Phys. Rept. **50** (1979) 157.

[5] B. Z. Kopeliovich, I. K. Potashnikova, I. Schmidt, Braz. J. Phys. **37**, 473-483 (2007). [arXiv:hep-ph/0604097 [hep-ph]].

[6] B. Z. Kopeliovich, I. K. Potashnikova, I. Schmidt, A. V. Tarasov, Phys. Rev. **D74**, 114024 (2006).

[7] R. S. Pasechnik and B. Z. Kopeliovich, Eur. Phys. J. C **71**, 1827 (2011) [arXiv:1109.6695 [hep-ph]].
[8] R. Pasechnik, B. Kopeliovich and I. Potashnikova, Phys. Rev. D **86**, 114039 (2012) [arXiv:1204.6477 [hep-ph]].
[9] B. Z. Kopeliovich, I. K. Potashnikova, I. Schmidt and A. V. Tarasov, Phys. Rev. D **76**, 034019 (2007) [hep-ph/0702106 [HEP-PH]].
[10] B. Z. Kopeliovich and B. Povh, Z. Phys. A **356**, 467 (1997) [nucl-th/9607035].
[11] B. Z. Kopeliovich, L. I. Lapidus and A. B. Zamolodchikov, JETP Lett. **33**, 595-597 (1981).
[12] G. Ingelman, P. E. Schlein, Phys. Lett. **B152** 256 (1985).
[13] J. C. Collins, D. E. Soper and G. F. Sterman, Adv. Ser. Direct. High Energy Phys. **5**, 1 (1989) [hep-ph/0409313].
[14] A. Brandt et al. [UA8 Collaboration], Phys. Lett. B**297**, 417 (1992).
[15] R. Bonino et al. [UA8 Collaboration], Phys. Lett. B**211**, 239 (1988).
[16] F. Abe *et al.* [CDF Collaboration], Phys. Rev. Lett. **78**, 2698 (1997) [hep-ex/9703010].
[17] T. Aaltonen *et al.* [CDF Collaboration], Phys. Rev. D **82**, 112004 (2010) [arXiv:1007.5048 [hep-ex]].
[18] K. A. Goulianos, hep-ph/9708217.
[19] G. Kubasiak and A. Szczurek, Phys. Rev. D **84**, 014005 (2011) [arXiv:1103.6230 [hep-ph]].
[20] M. B. Gay Ducati, M. M. Machado and M. V. T. Machado, Phys. Rev. D **75**, 114013 (2007) [hep-ph/0703315].
[21] R. Pasechnik, B. Z. Kopeliovich and I. K. Potashnikova, arXiv:1403.2014 [hep-ph].
[22] M. G. Ryskin, A. D. Martin, V. A. Khoze, Eur. Phys. J. **C60**, 265-272 (2009) [arXiv:0812.2413 [hep-ph]].
[23] M. G. Ryskin, A. D. Martin and V. A. Khoze, Eur. Phys. J. C **71**, 1617 (2011) [arXiv:1102.2844 [hep-ph]].
[24] B. Z. Kopeliovich, A. Schäfer and A. V. Tarasov, Phys. Rev. **D62**, 054022 (2000) [arXiv:hep-ph/9908245].
[25] B. Z. Kopeliovich and L. I. Lapidus, Pisma Zh. Eksp. Teor. Fiz. **28**, 664 (1978).
[26] H. I. Miettinen and J. Pumplin, Phys. Rev. D **18**, 1696 (1978).
[27] K. J. Golec-Biernat, M. Wusthoff, Phys. Rev. **D59**, 014017 (1998). [hep-ph/9807513].
[28] J. D. Bjorken, J. B. Kogut and D. E. Soper, Phys. Rev. D **3**, 1382 (1971).
[29] J. Bartels, K. J. Golec-Biernat and H. Kowalski, Phys. Rev. D **66** (2002) 014001.
[30] R. M. Barnett *et al.*, Rev. Mod. Phys. 68, 611 (1996).
[31] S. Amendolia *et al.*, Nucl. Phys. **B277**, 186 (1986).
[32] B. Z. Kopeliovich, H. J. Pirner, A. H. Rezaeian and I. Schmidt, Phys. Rev. D **77**, 034011 (2008) [arXiv:0711.3010 [hep-ph]].
[33] B. Z. Kopeliovich, I. K. Potashnikova, I. Schmidt and J. Soffer, Phys. Rev. D **78**, 014031 (2008) [arXiv:0805.4534 [hep-ph]].
[34] B. Z. Kopeliovich, A. H. Rezaeian, I. Schmidt, Phys. Rev. **D78**, 114009 (2008) [arXiv:0809.4327 [hep-ph]].
[35] B. Z. Kopeliovich, J. Raufeisen, A. V. Tarasov, Phys. Lett. **B503**, 91-98 (2001). [hep-ph/0012035].
[36] A. Donnachie, P. V. Landshoff, Nucl. Phys. **B303**, 634 (1988).
[37] G. Bertsch, S. J. Brodsky, A. S. Goldhaber, J. F. Gunion, Phys. Rev. Lett. **47**, 297 (1981).
[38] B. Z. Kopeliovich, proc. of the workshop Hirschegg 95: Dynamical Properties of Hadrons in Nuclear Matter, Hirschegg January 16-21, 1995, ed. by H. Feldmeyer and W. Nörenberg,

Darmstadt, 1995, p. 102 (hep-ph/9609385);
[39] S. J. Brodsky, A. Hebecker, and E. Quack, Phys. Rev. **D55** (1997) 2584.
[40] B. Z. Kopeliovich, A. V. Tarasov and A. Schafer, Phys. Rev. C **59**, 1609 (1999) [hep-ph/9808378].
[41] J. Raufeisen, J. -C. Peng and G. C. Nayak, Phys. Rev. D **66**, 034024 (2002) [hep-ph/0204095].
[42] S. J. Brodsky and P. Hoyer, Phys. Lett. B **298**, 165 (1993) [hep-ph/9210262].
[43] L. D. Landau, I. Ya. Pomeranchuk, ZhETF, 505 (1953).
[44] J. C. Collins, L. Frankfurt, M. Strikman, Phys. Lett. **B307**, 161-168 (1993) [hep-ph/9212212].
[45] J. C. Collins, Phys. Rev. **D57**, 3051-3056 (1998) [hep-ph/9709499].
[46] B. Z. Kopeliovich, I. K. Potashnikova, B. Povh and E. Predazzi, Phys. Rev. Lett. **85**, 507 (2000) [hep-ph/0002241].
[47] B. Z. Kopeliovich, I. K. Potashnikova, B. Povh and E. Predazzi, Phys. Rev. D **63**, 054001 (2001) [hep-ph/0009008].
[48] B. Z. Kopeliovich, I. K. Potashnikova, I. Schmidt, M. Siddikov, Phys. Rev. **C84**, 024608 (2011) [arXiv:1105.1711 [hep-ph]].
[49] T. Schäfer, E.V. Shuryak, Rev. Mod. Phys. **70**, 323 (1998).
[50] E. V. Shuryak and I. Zahed, Phys. Rev. D **69**, 014011 (2004) [hep-ph/0307103].
[51] B. Z. Kopeliovich, I. K. Potashnikova, B. Povh and I. Schmidt, Phys. Rev. D **76** (2007) 094020 [arXiv:0708.3636 [hep-ph]].
[52] A. H. Mueller and B. Patel, Nucl. Phys. B **425**, 471 (1994) [hep-ph/9403256].
[53] N. N. Nikolaev and B. G. Zakharov, J. Exp. Theor. Phys. **78**, 598 (1994).
[54] B. Z. Kopeliovich, I. K. Potashnikova, B. Povh and I. Schmidt, Phys. Rev. D **85**, 114025 (2012) [arXiv:1205.0067 [hep-ph]].
[55] S. Chekanov *et al.* [ZEUS Collaboration], PMC Phys. A **1**, 6 (2007) [arXiv:0708.1478 [hep-ex]].
[56] J. Bartels, S. Bondarenko, K. Kutak and L. Motyka, Phys. Rev. D **73** (2006) 093004 [hep-ph/0601128].
[57] J. Bartels, S. Bondarenko, K. Kutak and L. Motyka, Phys. Rev. **D73**, 093004 (2006).
[58] K. Wijesooriya, P. E. Reimer and R. J. Holt, Phys. Rev. C **72**, 065203 (2005) [nucl-ex/0509012].
[59] B. Z. Kopeliovich, J. Nemchik, I. K. Potashnikova, M. B. Johnson and I. Schmidt, Phys. Rev. C **72**, 054606 (2005) [hep-ph/0501260].
[60] A. Donnachie and P. V. Landshoff, Nucl. Phys. B **303**, 634 (1988).
[61] B. Z. Kopeliovich and A. V. Tarasov, Nucl. Phys. A **710**, 180 (2002) [hep-ph/0205151].
[62] J. F. Gunion and G. Bertsch, Phys. Rev. D **25**, 746 (1982).
[63] M. H. L. S. Wang, M. C. Berisso, D. C. Christian, J. Felix, A. Gara, E. Gottschalk, G. Gutierrez and E. P. Hartouni *et al.*, Phys. Rev. Lett. **87**, 082002 (2001).
[64] T. Affolder *et al.* [CDF Collaboration], Phys. Rev. Lett. **84**, 232 (2000).
[65] V. A. Khoze, A. D. Martin and M. G. Ryskin, Phys. Lett. **B401** (1997) 330;
[66] V. A. Khoze, A. D. Martin and M. G. Ryskin, Eur. Phys. J. **C14** (2000) 525;
[67] V. A. Khoze, A. D. Martin and M. G. Ryskin, Eur. Phys. J. **C19** (2001) 477 [Erratum-ibid. **C20** (2001) 599];
[68] V. A. Khoze, A. D. Martin and M. G. Ryskin, Eur. Phys. J. **C23** (2002) 311;
[69] A. B. Kaidalov, V. A. Khoze, A. D. Martin and M. G. Ryskin, Eur. Phys. J. **C33** (2004) 261.
[70] S. Heinemeyer, V. A. Khoze, M. G. Ryskin, W. J. Stirling, M. Tasevsky and G. Weiglein, Eur. Phys. J. C **53**, 231 (2008) [arXiv:0708.3052 [hep-ph]].
[71] S. Heinemeyer, V. A. Khoze, M. G. Ryskin, M. Tasevsky and G. Weiglein, Eur. Phys. J. C

71, 1649 (2011) [arXiv:1012.5007 [hep-ph]].
[72] M. Tasevsky, Eur. Phys. J. C **73**, 2672 (2013) [arXiv:1309.7772 [hep-ph]].
[73] G. Aad *et al.* [ATLAS Collaboration], Phys. Lett. B **716**, 1 (2012) [arXiv:1207.7214 [hep-ex]].
[74] S. Chatrchyan *et al.* [CMS Collaboration], Phys. Lett. B **716**, 30 (2012) [arXiv:1207.7235 [hep-ex]].
[75] M. S. Carena and H. E. Haber, Prog. Part. Nucl. Phys. **50**, 63 (2003) [hep-ph/0208209].
[76] S. Dittmaier *et al.* [LHC Higgs Cross Section Working Group Collaboration], arXiv:1101.0593 [hep-ph].
[77] S. Dittmaier *et al.* [LHC Higgs Cross Section Working Group Collaboration], arXiv:1201.3084 [hep-ph].
[78] S. Heinemeyer *et al.*, arXiv:1307.1347 [hep-ph].
[79] S. J. Brodsky, A. S. Goldhaber, B. Z. Kopeliovich and I. Schmidt, Nucl. Phys. B **807**, 334 (2009) [arXiv:0707.4658 [hep-ph]].
[80] S. J. Brodsky, B. Kopeliovich, I. Schmidt and J. Soffer, Phys. Rev. D **73**, 113005 (2006).